Biocatalysis and Agricultural Biotechnology 69 (2025) 103823

Contents lists available at ScienceDirect

Biocatalysis and Agricultural Biotechnology

journal homepage: www.elsevier.com/locate/bab

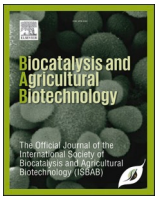

Dual anti-inflammatory and antioxidant potentials of *Balanophora fungosa* J.R. Forst. & G. Forst.: Computational predictions and *in vivo* validation

Gowtham Kannan [a], Benedict Mathews Paul [a], Madhu Bala Durairajan [a], Yamuna Annadurai [b], Shanmughavel Piramanayagam [c], Parimelazhagan Thangaraj [a,*]

[a] *Bioprospecting Laboratory, Department of Botany, Bharathiar University, Coimbatore, 641046, Tamil Nadu, India*
[b] *Post Doctoral Research Associate, Central Research Laboratory for Biomedical Research, Vinayaka Missions Medical College and Hospital, Karaikal, Puducherry, 609609, India*
[c] *ICMR-Adjunct Faculty, Department of Botany, Bharathiar University, Coimbatore, 641046, Tamil Nadu, India*

ARTICLE INFO

Keywords:
Balanophora fungosa
Inflammation
LC-TOF-MS
Oedema
Molecular dynamics
Bioaccessibility

ABSTRACT

Balanophora fungosa J.R. Forst. & G. Forst. is one amongst the 23 species of its genus with traditional claims in curing gastric discomfort, inflammation, wound healing, syphilis, gonorrhoea, and injuries due to falls, but unfortunately, with no scientific validation for its pharmacological properties. Hence, the current study aims to assess the comprehensive bioactivity profile by standard *in vitro* and *in silico* (Schrodinger) methods, and includes LC-TOF-MS analysis and FTIR for identification of the bioactive compounds. *In vivo* analysis was carried out in Wistar albino rats by the croton oil-induced ear oedema model. Among the screened extracts, *B. fungosa* methanolic extract, which showed superior bioactivity, has been analysed in an *in vitro* and *in silico* environment. The bio-accessibility levels of the anti-oxidative phyto-compounds above the superlative levels (>100 %) show the therapeutic and consumable quotient of *B. fungosa* crude extracts. Furthermore, its molecular interactions amongst inflammation receptor proteins and lead bioactive compounds identified through LC-TOF-MS and validated by HPLC showed remarkable binding affinities with a dock score as high as −12.81 kcal/mol and −11.24 kcal/mol with TNF-α and NF-kB receptor proteins, respectively, higher than the dock scores of Diclofenac and Aspirin. All the docked complexes showed stable interaction with RMSD ranging between 1.5 and 2.8 Å over a 100 ns simulation, wherein NFkB-Balanophotannin A complex showed the highest binding free energy of −147.55 kcal/mol. *In vivo* analysis also revealed a distinctive reduction of inflammatory oedema (85.35 %) by *B. fungosa* methanolic extract in a dose-dependent manner, affirming its ethnomedicinal use in treating inflammation.

1. Introduction

Inflammation is a complex biological response to infection, injury, or metabolic stress and is critical for restoring homeostasis.

* Corresponding author. Department of Botany Bharathiar University, Coimbatore, 641 046, Tamil Nadu, India
E-mail address: drparimel@gmail.com (P. Thangaraj).

https://doi.org/10.1016/j.bcab.2025.103823
Received 14 April 2025; Received in revised form 5 October 2025; Accepted 12 October 2025
Available online 14 October 2025

However, chronic or dysregulated inflammation contributes to the development and progression of numerous diseases such as diabetes, atherosclerosis, neurodegenerative disorders, and cancer (Paul et al., 2024). A pivotal driver of this pathological inflammation is oxidative stress, characterized by excessive production of reactive oxygen species (ROS), which activate multiple intracellular signaling pathways. This redox imbalance leads to the activation of key transcriptional and signaling mediators, triggering a cascade of pro-inflammatory responses (Dietz et al., 2016).

Among the molecular players involved, Nuclear Factor Kappa B (NF-κB) serves as a central regulator of inflammation. Upon activation by stimuli such as ROS, cytokines, or microbial components, NF-κB translocates to the nucleus and upregulates the expression of pro-inflammatory genes, including Tumor Necrosis Factor-alpha (TNF-α), Interleukin-6 (IL-6), and Cyclooxygenase-2 (COX-2) (Azam et al., 2024; Kannan et al., 2025). These effectors further amplify the inflammatory response, leading to tissue damage and chronic inflammatory conditions.

Toll-Like Receptor 6 (TLR6), part of the innate immune system, recognizes pathogen-associated molecular patterns (PAMPs) and forms heterodimers with TLR2 to trigger downstream signaling. Upon activation, TLR6 engages the MyD88-dependent pathway, culminating in the activation of NF-κB and mitogen-activated protein kinases (MAPKs), which in turn enhance transcription of TNF-α, IL-6, and COX-2 (Amin et al., 2022). Thus, TLR6 acts upstream in the signaling hierarchy, acting as a crucial sensor and amplifier of inflammation.

TNF-α, a key pro-inflammatory cytokine, further propagates the inflammatory response by stimulating the NF-κB pathway in an autocrine and paracrine manner, sustaining the production of additional inflammatory mediators. Simultaneously, IL-6, another major cytokine induced by NF-κB, plays a dual role—while it helps in acute immune responses, its persistent expression is linked to chronic inflammation and tissue remodeling (Nangap et al., 2024).

COX-2, an inducible isoform of cyclooxygenase, catalyzes the conversion of arachidonic acid into prostaglandins, particularly prostaglandin E2 (PGE2), which promotes vasodilation, oedema, and pain. COX-2 expression is directly upregulated by NF-κB and reinforced by IL-6 and TNF-α, closing a feedback loop that exacerbates inflammation (Surh, 2011).

Given the interconnected nature of these mediators, targeting this network offers a promising strategy for anti-inflammatory therapy. In this light, plant-derived phytochemicals such as glycyrrhizin, hesperidin, and myricetin with dual antioxidant and anti-inflammatory capacities are gaining attention for their ability to modulate these molecular pathways effectively (Srivastava et al., 2024).

One such plant is *Balanophora fungosa* J.R. Forst. & G. Forst., a wild, chlorophyll-lacking, ethnomedicinal species native to the Western Ghats, particularly the Keelkothagiri region. Known locally as Fungus Root (*Bhoomi Budalam*), it belongs to the family Balanophoraceae and is traditionally consumed in the Kolli hills as a wild edible with hepatoprotective and antipyretic uses (Ranjithakani et al., 1992). Despite its traditional use in tribal communities of the Kothagiri region for reducing swellings and pain, scientific validation of its bioactive potential remains unexplored, which the current study seeks to report.

Encouragingly, two new butenolides and balanolides isolated from *B. fungosa* have shown anti-inflammatory activity in RAW 264.7 macrophage lines, a standard model for studying cytokine and prostaglandin release (Zhou et al., 2021). Moreover, Huu Tai et al. (2020) identified three new muurolane-type sesquiterpene glycosides from *B. fungosa* with cytotoxic potential. A recent comprehensive review by Mutinda et al. (2023) highlighted that related species—including *B. laxiflora*, *B. abbreviata*, *B. involucrata*, and *B. indica*—share anti-inflammatory properties, indicating the broader therapeutic relevance of this genus (Nguyen et al., 2022; Luo et al., 2007; Pan et al., 2008).

Nonetheless, current literature lacks integrated pharmacological and computational studies evaluating *B. fungosa*'s effects on key inflammatory mediators such as NF-κB, TLR6, TNF-α, IL-6, and COX-2. The absence of ADMET profiling and target-specific validation creates a significant research gap.

This study hypothesizes that *B. fungosa* phytocompounds mitigate inflammation and oxidative stress by modulating core inflammatory mediators and signaling pathways. Through a bioassay-guided approach combining *in vivo* animal models and *in silico* docking with ADMET profiling, we aim to validate its potential as a dual-action anti-inflammatory and antioxidant therapeutic, bridging traditional ethnomedicine with modern pharmacological science that lays the baseline for future mechanistic and translational research.

2. Materials and methods

2.1. Chemicals and reagents

All the chemicals used in this study were of analytical grade and purchased from HiMedia Laboratories, Mumbai, and Sigma Aldrich, USA. Solvents were of HPLC grade and purchased from Merck Millipore (Bangalore, India). Milli-Q water (Merck Millipore; Billerica, MA, USA), which had a total oxidizable carbon value of less than 5 ppb and a resistivity of 18.2 MΩ cm^{-1} at 25 °C, was utilised for all conducted experiments.

2.2. Collection and identification of Balanophora fungosa

The whole plant of *B. fungosa* J.R. Forst. & G. Forst. was collected during June from the Shola Forest of Kothagiri, Ooty District, Tamil Nadu, India. The specimens were identified and authenticated [BSI/SRC/5/23/2022/TECH/666] by the Botanical Survey of India, Coimbatore.

2.3. Processing and extraction of B. fungosa

To remove dirt particles and contaminants that had adhered, the aerial parts of *B. fungosa* were repeatedly washed with tap water and then distilled water. Subsequently, the plant portions were chopped into pieces and left to dry in the shade at room temperature. After drying, the powdered sample, pulverised using a mixer grinder (Sujata Dynamix-810W; Delhi, India), was weighed using a digital balance (Shimadzu, Japan), and kept at −20 °C for further tests. Subsequently, a thimble with the powdered sample is packed and extracted using a hot percolation technique, sequentially using organic solvents (petroleum ether, ethyl acetate, methanol, and water), maintained at their respective boiling temperatures to facilitate extraction. The plant material thimble was dried at 40 °C in a hot air oven before the change of solvents. The extracts were then concentrated using a rotary vacuum evaporator (Equitron Ev11-ABS.051, India), and all the solvent extracts were allowed to air dry (Nataraj et al., 2023). The dried extracts of petroleum ether, ethyl acetate, methanol, and water (BFPE, BFEA, BFME, and BFAE) were kept at −20 °C for future experiments to ensure there is no loss in their integrity. Further, its recovery % was calculated using the following Equation (1).

2.4. Screening of phytochemical compounds of B. fungosa

The dry powder of *B. fungosa* aerial parts was subjected to preliminary screening of phytochemicals based on the methods of Durairajan et al. (2024), elaborated in Supplementary Protocol 1. Based on the intensity of the colour developed in the experiments, the presence and absence of phytochemicals were confirmed.

2.5. Estimation of primary and secondary metabolites

The quantification of macromolecules such as carbohydrates, proteins, and amino acids is essential for estimating the nutritional quality of the raw plant samples, which are expected to be palatable and a potent medicinal product. These primary metabolites are considered to improve the medicinal value of the products developed from the plant samples. Hence, the primary metabolites (carbohydrates, proteins, and amino acids) were estimated in 100 mg of shade-dried samples, and secondary metabolites (phenolics, flavonoids, and tannins), which can exert bioactivity in our body system, were quantified in 100 μg of extracts. All the quantification methods adhered to standard protocols (Parimelazhagan, 2015), detailed in Supplementary Protocols 2–7.

2.6. Antioxidant activity

The antioxidant potential of *B. fungosa* extracts (Petroleum ether, ethyl acetate, methanol, water) at 100 μg/mL concentration was determined through scavenging of non-physiological free radicals such as DPPH (2,2-diphenyl-1-picrylhydrazyl), Phosphomolybdenum reduction, FRAP (Ferric Reducing Antioxidant Power), and superoxide following standard protocols (Parimelazhagan, 2015) detailed in Supplementary Protocols 8–11.

2.7. Screening of bioactive extract through anti-inflammatory analysis

The anti-inflammatory effect refers to the ability of a medication or chemical to lessen inflammation that prevents 5-Lipoxygenase. The bioassay commonly used to predict the anti-inflammatory efficacy of plant extracts is 5-Lipoxygenase (5-LOX) enzyme inhibition (Supplementary Protocol 12). This enzyme catalyzes the oxidation of arachidonic acid to produce leukotrienes, which are potent inflammatory mediators that promote asthma and arthritis as well as various other localized or systemic inflammatory conditions. Given the well-known critical role of leukotrienes in inflammatory responses, we propose that counteracting overexpression by acting on 5-LOX can yield significant anti-inflammatory effects. In addition, the suppression of 5-LOX suggests that it might have a more diverse pharmacological profile involving immunomodulation and/or antioxidant properties. Some plant extracts and phytochemicals, such as terpenoids, alkaloids flavonoids, are good 5-LOX inhibitors; therefore, they were expected to serve as anti-inflammatory agents. It has been a cornerstone of discovery research into new anti-inflammatory substances in pharmacognosy, phytochemistry, and ethnopharmacology investigations, as well as for confirming the traditional medical uses of plants to prevent or alleviate inflammation (DSVGK et al., 2014). Natural anti-inflammatory compound, Curcumin, was used to compare the therapeutic effect of the plant extracts. Appropriate dilutions of test samples were used to determine the 5-LOX activity. In addition, the membrane stabilization method as a parameter assay to assess anti-inflammatory activity was also performed on the bioactive extract, and the concurrent percentage of inhibition was estimated (Supplementary Protocol 13). The membrane stabilization method (Shinde et al., 1999) is another most sought *in vitro* procedure for the anti-inflammatory activity of medicinal plants. This is associated with the concept that some anti-inflammatory agents will work equally by stabilization of cell membranes, and therefore it enhances reducing or preventing elimination (breakdown) of cells, as well as releasing inflammation creators. Cell membrane, especially that of red blood cell (RBC), is soft to lyse under conditions like hypotonicity or heating stress. Lysis of cells results in the release of cellular contents, which includes inflammatory mediators like histamines, cytokines, and other pro-inflammatory molecules. The second is via the membrane stabilization process, which requires maintenance of cell wall integrity through means of administration by anti-inflammatory products, which would stabilize or protect cells from stresses sufficiently to prevent lysis and release of inflammatory mediators (Khatun et al., 2024).

2.8. Bio-accessibility of antioxidant potential and phyto-constituents release

The bio-accessibility (BA) of the phyto-constituents release and antioxidant potential were assessed using the international consensus model INFOGEST (Minekus et al., 2014). The INFOGEST model is an *in vitro* digestion assay that models the human gastrointestinal tract, established by COST Action INFOGEST, and widely applied to test the selectivity of plant extracts for their bio-accessibility and/or antioxidant capacity. The test simulator is designed to replicate the physiological elements of enzymatic digestion in adults, covering oral, gastric, and intestinal phases and their respective enzymes at a definite pH and temperature, making it a repeatable and standardized procedure for controlled assessments. The bioavailability of several plant extracts, as well as the potential absorption and release by *in silico* methods, were investigated for polyphenols, flavonoids, and antioxidants using this model. INFOGEST can simulate the digestive process and predict what bioactive compounds in the food matrix would probably be absorbed by people, as well, how much. Identification of the antioxidant, anti-inflammatory, and health-promoting effects of plant extracts provides valuable information, necessary for the design and discovery of functional foods/nutraceuticals/plant therapeutics (Brodkorb et al., 2019). Each phase of digestion was carried out (Supplementary Protocol 14), and the total phytoconstituents release and antioxidant activity of the digested samples were determined to finally derive the bio accessibility index (BAI) percentage, which was calculated as per Equation (2).

2.9. Assessment of functional groups of bioactive extract using ATR-FTIR

The frequency range between 4000 and 600 cm^{-1} was set to acquire the FTIR spectral image of BFME using an Attenuated Total Reflectance – Fourier Transform Infrared (ATR – FTIR) Spectrometer (Model: JASCO FT/IR 4700, Japan) equipped with a DLaTGS detector with an aperture size of 50 × 50 μm; 100 times accumulation under transmission measurement method. The acquired spectrum was further analysed to find the chemical groups associated with the phytochemical constituents and to identify the molecule's backbone or the functional groups connected inside the sample, including the type of functional groups, including distinguishing linear/branched or saturation/unsaturation/aromatic chains and rings in the chemical structure present in the fingerprint region and double, triple and single bond areas. The derived peaks were compared to the reference database (Socrates, 2004; Nandiyanto et al., 2019).

2.10. LC–TOF–MS analysis of bioactive extract

In order to identify the bioactive components of BFME, an Agilent Jet Stream Thermal Gradient Technology system, an Agilent 1290 Infinity Liquid Chromatography (LC) System was connected to an Agilent 6545 accurate-mass quadrupole time-of-flight (Q-TOF) apparatus. The chromatographic method was selected based on the gradient (0–20 min, 10–100 % B; 22–25 min, 10 % B; flow 0.5 ml/min), injection volume (10 μL), flow rate (0.5 mL/min), and composition of the mobile phase [10 mM ammonium acetate in water (A) and acetonitrile (B)] (Chanda et al., 2020). The optimization was carried out by modifying certain parameters, such as drying gas flow, drying gas temperature, nebulizer gas pressure, capillary voltage, skimmer voltage, and nozzle voltage, to improve the resolution, analysis time, and peak shape. High-resolution accurate mass analysis was used to identify the compounds; this corresponds to a score value (on a scale of 0–100) of the measured mass (m/z) with respect to their theoretical formula. Improved tandem mass spectra and high-resolution mass spectra under MS conditions were obtained by using the negative ion mode. Prior to the analysis, the mass axis of the TOF was calibrated by recording the real flight durations for ions of known masses after a sample with known masses was injected into the source. Agilent MassHunter Acquisition B.06.01 software (Agilent Technologies, Santa Clara, CA, USA) was used to collect data from the LC/Q-TOF. Agilent MassHunter Qualitative Analysis B.07.00 (MassHunterQual, Agilent Technologies, Santa Clara, CA, USA) was utilised to deconvolve the data into individual chemical peaks using Molecular Feature Extractor. MassHunter Acquisition B.06. 01 combines data acquisition in real time with optimal tuning settings using results as input to detect the analytes precisely and accurately on mass spectrometers. It works with all of MS techniques from single quadrupole to high-resolution mass spectrometry. At the same time, MassHunter Qualitative Analysis B.07.00 delivers advanced data processing for identifying, quantifying, and analyzing compounds within complex samples. When used in tandem, these software solutions increase analytical accuracy and dependability while streamlining the process (Mamani-Huanca et al., 2022). Creating a unique database and importing it into the MassHunterQual software's algorithm that included molecular feature extraction, find by formula, recursive feature extraction, and mass profiler professional integration algorithms resulted in focused data mining, which allowed for the identification of the substance (Mamani-Huanca et al., 2021).

2.11. Validation and quantification of BRME compounds by HPLC analysis

The *B. fungosa* methanolic extract was subjected to HPLC analysis to validate and quantify the bioactive compounds identified in LC-TOF-MS analysis. The analysis was carried out in a Shimadzu preparative cum analytical HPLC system (Shimadzu Corporation, Kyoto, Japan) equipped with a binary solvent pump (LC 20 AP) coupled to a photodiode array detector (PDA) (SPD N 20A) with a C18 column (5 μm, Dimension- 4.6 × 250 mm). Data were processed using Lab SolutionsTM software (Shimadzu Corporation, Kyoto, Japan).

The following method was standardized to elute polyphenolic compounds. Mobile phase consisted of Solvent A: Water with 0.1 % Trifluoro acetic acid and Solvent B: Acetonitrile; The gradient was set for Pump B concentration to time as follows: 15 % - 1 min; 30 % - 10 min; 50 % - 15 min; 60 % - 20 min; 75 % - 25 min; 80 % - 30 min; 30 % - 35 min; 15 % - 37 min; 0 % - 40 min. The total duration was

set at 40 min at a 0.8 mL/min elution rate and 15 μL injection volume. The temperature of the oven was maintained at 40 °C. All the reference standard compounds (5 mg/mL) were dissolved in HPLC-grade methanol and filtered using 0.45 μmsyringe filters. The quantity of the compounds present in the extract was determined using the following formula.

$$C_{(sa)} = [C_{(st)} \times A_{(sa)}]/A_{(st)}. \quad \text{Equation 3}$$

$C_{(sa)}$ = Concentration of compound in sample; $C_{(st)}$ = Concentration of standard; $A_{(sa)}$ = Peak area of sample; $A_{(st)}$ = Peak area of standard.

2.12. In silico docking for binding efficacy with anti-inflammatory proteins

Docking calculations were carried out on Schrödinger Suite v2023. Common inflammatory marker proteins such as NF-kB protein (PDB ID:1VKX), TNF-α receptor (PDB ID: 3GIO), Interleukin 6 receptor (PDB ID: 1I1R), TLR-6 receptor (PDB ID: 4OM7), and COX-1 receptor (PDB ID: 3KK6) were selected based on the following criteria:

- High resolution of the crystal structure to ensure accurate docking (≤3.0 Å).
- Completeness of the binding domain or functional region relevant to ligand binding with no pre-existing mutations in the protein.
- Relevance of the co-crystallized ligand or conformational state (active/inactive) to our study.

The 3-D protein structure was downloaded from the Research Collaboratory for Structural Bioinformatics Protein Data Bank [RCSB-PDB] (Goodsell et al., 2020). :The protein preparation wizard was employed to prepare the proteins by removing all the water molecules and adding hydrogen ions. pH was fixed to be 7.0. Small molecules that were bound to the crystallized structure of proteins were removed. Energy minimization was done for all the protein structures. Grid box dimensions were generated using the axis co-ordinates listed in Supplementary Table 4.

3D structures in.sdf file format were retrieved from the PubChem database for the 19 small compounds obtained from LC-TOF-MS analysis. All 19 retrieved structures were run on LigPrep of the GLIDE module as a ligand preparation protocol. GLIDE Module, a subset that is vital for molecular docking experiments, and it allows the user to predict how small molecules may dock into a protein target. Using flexible ligand and receptor conformations, it generates precision docking results that leadit to a key role in drug discovery and structure-based design (Sandor et al., 2010). As a result, 573 stereoisomers were secured. Electrostatic potential was calculated, and Gasteiger charges were added according to the free energy. The receptor grid generation panel was used to set the grid around the target proteins. Active site prediction was performed using PrankWeb (https://prankweb.cz/), which identifies ligand-binding pockets based on a combination of residue conservation, surface topology, and physicochemical properties. The pockets were ranked by a deep learning-based score (DL score), and the highest-scoring pocket was selected for molecular docking studies. Ligand docking was performed for four proteins with 573 small molecule stereoisomers, and the results were visualized with XP-visualizer, which is an essential tool for the high precision results analysis and visualization of molecular docking. An additional asset to this tool is the ability for a user to inspect in greater detail ligand-receptor interactions, including both hydrogen bonds and hydrophobic contacts (σ-interactions), helping one better understand binding modes as well as facilitating hit-to-lead optimization (Saxena et al., 2018; Rajagopal et al., 2020). The docking results of the BFME compounds with target proteins were compared with the docking profile of standard anti-inflammatory drugs, Diclofenac (PubChem ID: 3033) and Aspirin (PubChem ID: 2244), following the same parameters followed previously.

2.13. Molecular dynamics simulation

The Molecular Dynamics Simulation was performed to validate the docking profile of the five inflammatory proteins using the Desmond module of Schrodinger (version 12.3) software package (Annadurai et al., 2023) for 100ns each. Preliminarily, the target proteins were pre-processed and optimized using a protein preparation workflow. System builder is used to set the requisite parameters as temperature, pressure, and neutralization, for MD simulation analysis.

Ortho-rhombic-shaped boundaries were set to run the dynamic simulation, and it was filled with the TIP3P water model with three inflexible atoms each, which allocated the Lennard-Jones parameters and charges. For all five proteins, the salt concentration (Na + ions) was 0.15 M, pressure at 1.01325 bars, and temperature was maintained at 300 K, and the protein-ligand complex was simulated in a water medium for 100 ns, with every 100 ps trajectories saved for future analysis. The Desmond minimization panel executed the Brownian motion of the system at low temperature (10 K) in a quick manner. The following parameters were observed and optimized for each protein specifically:

For the NFκB – Balanophotannin - A complex, box volume was 1040298 A^3 and total observed atoms in simulation was 98082; For TNF-α - Balanophotannin - A complex, box volume volume was 423534 A^3 and the system was neutralized with 1 Cl-ion, further 39447 atoms was run on simulation; IL6 - Balanophotannin complex, set towards 1066694 A^3, volumetric box and neutralized by adding 9 Na + ions. The total atoms in the simulation was 100723; TLR6–p–Coumaric acid complex was set into an orthorhombic-shaped box with 352261 A^3 volume and neutralized by adding 1 Cl-ion. 32791 atoms were fixed into a water model for dynamic simulation. For the simulation of COX1 - Ellagic acid complex, the system was set into a 1109547 A^3 volumebox and neutralized by the addition of 4 Cl-ions. A total of 135123 atoms were found to be in the simulation. Simulations of all five complexes were done with the TIP3P water model. Protein RMSD (Root Mean Square Deviation) was calculated witC-alpha(Red); Protein RMSF (Root Mean Square Fluctuation)

was also derived subsequently.

2.14. MMGBSA analysis

The binding free energy of each complex was calculated using the MMGBSA module of Schrodinger (Annadurai et al., 2023). Based on electrostatic, hydrophilic, and hydrophobic interactions, binding free energy was calculated using the following formula:

ΔG_{Sol} – Difference between GBSA solvation energy of the complex and the cumulative of individual solvation energy of the unbound protein & inhibitor.

ΔE_{mm} – Difference in minimised energies of the protein, ligand, and the complex, and the total energy of unbound protein & inhibitor.

ΔG_{SA} – Difference between the surface area energies of the complex and the cumulative individual surface area energy of an unbound protein and inhibitor.

2.15. ADMET analysis

The qIKProp module was used to evaluate the ADMET (Adsorption, Distribution, Metabolism, Excretion, and Toxicity) of 19 phytochemicals that were identified through LC-qTOF-MS analysis. This module is very important for predicting ADMET properties of compounds. It is reported on the predictor of 34 different physicochemical properties based on machine learning and which can be used by a researcher to predict the drug-likeness and further optimize for desired pharmacokinetic properties while designating novel chemical structures as potential drug candidates (Mali and Chaudhari, 2019). By using this ADMET test, adverse side effects and failure rates in the synthesis process, clinical trials, and labs can be prevented (Annadurai et al., 2023).

2.16. In vivo anti-inflammatory activity

The topical anti-inflammatory activity was evaluated as inhibition of the croton oil-induced ear oedema in Wistar albino rats (Tubaro et al., 1986). These rats were purchased from the Biogen Laboratory Animal Facility, Bangalore, India. Animals were categorized into six groups [Untreated control, positive control (Diclofenac at 10 mg/kg), Negative control, low dose (50 mg/kg), mid dose (100 mg/kg), and high dose (200 mg/kg)], each with six individual healthy rats (approximately 250 g normalized weight). The animals were housed in standard laboratory conditions with a 12-h light/dark cycle, temperature maintained at 22 ± 2 °C, and relative humidity of 50–60 %. They were given free access to a standard pellet diet and water ad libitum. Inflammation was always induced in the late morning (10.00–12.00 h). Mice were anaesthetised with ketamine hydrochloride (145 mg/kg, intraperitoneally) and an inflammatory response was induced on the inner surface of the right ear (surface: about 1 cm^2) by application of 80 g of croton oil suspended in 42 % aqueous ethanol. Negative control animals received only the irritant, whereas other animals received the irritant together with the tested substances (Diclofenac and *B. fungosa* extracts at different doses). At the maximum of the oedematous response, 6 h later, mice were sacrificed and both the treated (right) and the untreated (left) ears were removed. Oedema was measured as the weight difference between the two ears. The anti-inflammatory activity was expressed as a percentage of the oedema reduction in treated mice compared to the control mice using the equation below:

As a reference, the non-steroidal anti-inflammatory drug (NSAID), Diclofenac, was used as a positive control. All experimental procedures were conducted following institutional guidelines and were approved by the Institutional Animal Ethics Committee (IAEC) (Ethics No. KMCRET/ReRc/Ph.D/74/2023), which ensured the ethical compliance of the experiments and the guarantee of animal welfare.

2.17. Statistical analysis

The results were expressed as Mean ± Standard Deviation (n = 3). Using SPSS version 20.0, the data were statistically analysed using one-way ANOVA and Duncan's test. A value of $p < 0.05$ was deemed statistically significant for the mean values.

3. Results

3.1. Qualitative phytochemical screening

Primary and secondary metabolites, particularly carbohydrates, proteins, phenolics, flavonoids, tannins, gums and mucilages were found in the *B. fungosa* aerial part powder sample, however, they were dispersed differently across the plant, according to the preliminary phytochemical analysis (Supplementary Table 1).

3.2. Quantification of primary metabolites

The primary metabolites of *B. fungosa* aerial part powder samples (100 mg) were quantified using standard methods. The analysis resulted in a total carbohydrate level of 15.78 mg Glucose equivalents/g sample and a very high protein content of 142.95 mg Bovine Serum Albumin equivalents/g sample. The total amino acid level was also quantified, and it ranged to an extent of 102.62 mg Leucine equivalents/g sample.

3.3. Extract recovery percentage

After successive Soxhlet extraction with organic solvents, the maximum yield was obtained from the hot water (BEAE) and methanol (BFME) extracts, which were 23.45 % and 19 % of dried powder, respectively. The yield percentage in low polar solvents was comparatively very low (BFPE- 3.25 % and BFEA- 2.12 %).

3.4. Quantification of secondary metabolites

The secondary metabolite distribution in various extracts of *B. fungosa* is represented in Supplementary Table 2. Of all the extracts, ethyl acetate extract (BFEA) showed the highest levels of phenolics (145.36 mg Gallic acid equivalents/g extract), flavonoids (116.59 mg Rutin equivalents/g extract), and tannins (133.44 mg tannic acid equivalents/g extract), followed by the methanolic extract.

3.5. Antioxidant activity

From the analysis of *in vitro* antioxidant activity (Table 1), it was found that the BFEA sand BFME have better antioxidant capacity when compared to other extracts, especially in scavenging non-physiological free radicals such as DPPH, Superoxide, Ferric ions, and phosphomolybdenum complex. In DPPH radical scavenging activity, BFEA and BFME showed 74.2 % and 54.29 % scavenging activity and IC_{50} value of 19.156 μg/mL and 23.69 μg/mL respectively, while in superoxide radical scavenging activity, BFEA and BFME exhibited inhibition of 83.9 % and 79.4 %, respectively, which was comparable to the activity of reference compounds Butylated Hydroxy Toluene (BHT) and Rutin. In the Phosphomolybdenum reduction assay, also known as total antioxidant capacity assay, BFEA (23.3 mg AAEAC/g extract) and BFME (18.9 mg AAEAC/g extract) showed comparable reduction activity (BFEA-IC_{50} – 76.279 μg/mL; BFME-IC_{50}- 83.351 μg/mL). A similar trend was followed in the FRAP assay, where again BFEA showed competent ferric-reducing antioxidant activity (44.3 mM FEAC/mg extract).

3.6. Screening of bioactive extract by anti-inflammatory activity

Based on the antioxidant activity, BFEA and BFME were further compared for their anti-inflammatory potential through membrane stabilization and inhibition of 5-Lipoxygenase enzyme, which are the predominant approaches to select the best extract that can exert a therapeutic function against inflammation.

The erythrocyte membrane lysis caused by the hypotonic solution was considerably protected by BFME (50 μg/mL) in the membrane stabilization experiment, to an extent of 88.50 %, which is equivalent to the standard Diclofenac sodium (71.49 %). BFEA showed a comparable inhibition (80.02 %) against RBC membrane destabilization. While in the 5-Lipoxygenase enzyme inhibition assay, the methanol extract of *B. fungosa* (50 μg/mL) showed remarkable anti-inflammatory activity (89.06 % inhibition) based on the 5-Lipoxygenase (5-LOX) assay. The inhibitory percentage of the ethyl acetate extract and the standard curcumin were 79.97 % and 81.91 %, respectively. It can be seen that BFME and BFEA have shown 5-LOX inhibition greater than that of the standard Curcumin.

Hence, from the results of the anti-inflammatory potential analysis, *B. fungosa* methanolic extract (BFME) exhibited comparatively better anti-inflammatory activity than BFEA due to the presence of its anti-inflammatory compounds, including Balanophotannins, coumaric acid, ellagic acid, Brevifloin, Lupeol, Daucosterol, etc (Mutinda et al., 2023). Hence, BFME was investigated further to find out the constituent phytocompounds and their potent targets in inflammation.

3.7. Influence of bio-accessibility on antioxidant potential and phytoconstituents release

The bio-accessibility index (BAI) of antioxidant potential and phyto-metabolites release at different stages of digestion was analysed using a simulated gastro-intestinal (GI) digestion model and derived using Equation (2) in comparison with the crude extract's bioaccessibility (BA), considered to be 100 %. From the results of BAI of antioxidant potential (Table 2), at three phases i.e., oral, gastric and intestinal; as these prominent phases are the tripartite spots in digestion process where metabolic enzymes act upon the food matrix, it can be seen that, BFPE, BFEA and BFAE has moderately increased their BA of DPPH scavenging activity at intestinal phase to an extent of 109.53 %, 103.83 % and 118.93 % respectively while BFME has shown steady BA increase through all the phases with highest record at gastric phase (99.59 %). While in the scavenging of superoxide radicals, the BA of BFPE has shown the highest and lowest range at the gastric phase of BFPE (117.69 %) and oral phase (93.05 %), respectively. While all other extracts had maintained higher levels of BA in all phases, showing the scavenging ability on superoxide radicals between the ranges of 103.52–113.57 %. In nitric oxide radical scavenging potential, the BA has peaked to an extent of 148.20 % at the intestinal phase of BFPE. While the bioactive BFME and BFEA have shown optimum BA at the gastric phase, with a record of 124.11 % and 138.94 % respectively. BA of ABTS radical scavenging activity has shown steady maintenance of BA of BFME at all three phases to an extent of 99 % while the highest BA has been recorded by BFEA at its gastric phase (105.38 %). After taking into account the exuberant BAI of antioxidant potential of the BFPE, BFEA, and BFME extracts, it can be ascertained that BFME has shown a steady scavenging rate of the free radicals, while there has been a wide range of variation with every phase of BFPE and BFEA extracts. Unfortunately, BFAE has shown a lower BAI than other extracts, which shows the inability of BA to completely elute polar compounds during aqueous extraction.

From the results of the BAI of phyto-metabolite release (Table 2), the BA of carbohydrates and amino acids have shown a very high BAI above 100 %. The BAI of carbohydrates has reached a level of 978.74 % in the gastric phase of BFPE, while the lowest level of

Table 1
Antioxidant and anti-inflammatory activity of *B. fungosa* extracts Values are expressed as mean of triplicate determination (n = 3) ± standard deviation. The mean values were statistically significant at $p < 0.05$ where $^{a>b>c}$.

Sample (100 µg/mL)	DPPH radical scavenging activity (% inhibition)	Superoxide radical scavenging ability (% inhibition)	Phosphomolybdenum reducing ability (mg Ascorbic acid Equivalents antioxidant capacity/ g extract)	Ferric reducing antioxidant power (mM Ferrous Equivalents antioxidant capacity/g extract)	Membrane Stabilization method (% inhibition)	5 - Lipoxygenase inhibition method (% inhibition)
BFPE	26.02 ± 2.60 ^{d}	71.4 ± 1.86 ^{b}	15.65 ± 0.20 ^{b}	6.59 ± 5.57 ^{c}	72.01 ± 0.23 ^{b}	55.67 ± 1.33 ^{c}
BFEA	74.2 ± 0.43 ^{b}	83.9 ± 1.37 ^{a}	23.3 ± 0.22 ^{a}	44.3 ± 0.57 ^{a}	84.02 ± 0.32 ^{a}	81.97 ± 0.30 ^{a}
BFME	54.29 ± 2.42 ^{c}	79.44 ± 3.06 ^{a}	18.9 ± 0.15 ^{b}	36.08 ± 0.25 ^{b}	82.50 ± 0.40 ^{a}	82.06 ± 0.17 ^{a}
BFAE	44.08 ± 6.02 ^{c}	7.57 ± 1.19 ^{b}	16.66 ± 0.87 ^{c}	38.36 ± 0.24 ^{b}	71.44 ± 0.49 ^{b}	77.97 ± 0.87 ^{b}
Positive Control	***Rutin*** 92.7 ± 0.56^{a}	***Rutin*** 76.6 ± 0.68^{a}	–	–	***Diclofenac*** 71.49 ± 0.08 ^{a}	***Curcumin*** 81.91 ± 0.11 ^{a}
	BHT 88.6 ± 0.44^{a}	***BHT*** 41.4 ± 0.91^{c}	–	–		

Table 2
Bio-accessibility index of antioxidant potential and phyto-constituents release.

Sample	Phase of Digestion	Bio-accessibility Index (%)								
		DPPH radical scavenging activity	Superoxide radical scavenging activity	Nitric oxide radical scavenging activity	ABTS radical scavenging activity	Total Carbohydrates	Total Proteins	Total Amino acids	Total Phenolics	Total Flavonoids
BFPE	*Oral*	94.49 ± 1.00^{b}	93.05 ± 0.52^{b}	101.90 ± 0.24^{c}	100.80 ± 0.63^{a}	764.55 ± 0.68^{a}	109.41 ± 0.45^{b}	510.43 ± 0.82^{a}	58.60 ± 1.52^{b}	34.16 ± 1.51^{a}
	Gastric	107.85 ± 0.32^{a}	117.69 ± 0.88^{a}	146.83 ± 0.96^{a}	94.96 ± 0.47^{b}	978.74 ± 0.68^{a}	48.84 ± 0.22^{c}	323.06 ± 3.93^{a}	35.26 ± 0.28^{b}	26.34 ± 1.72^{b}
	Intestinal	109.53 ± 0.12^{a}	113.44 ± 0.69^{a}	148.20 ± 1.20^{a}	97.31 ± 0.35^{b}	169.81 ± 1.04^{c}	51.81 ± 1.20^{c}	894.91 ± 1.45^{a}	38.62 ± 0.15^{b}	35.28 ± 1.68^{a}
BFEA	*Oral*	109.75 ± 0.42^{a}	111.64 ± 1.67^{a}	130.41 ± 1.13^{a}	103.05 ± 1.04^{a}	59.95 ± 0.64^{d}	43.12 ± 2.02^{c}	294.57 ± 0.78^{b}	41.80 ± 0.38^{c}	26.77 ± 0.34^{b}
	Gastric	107.65 ± 0.97^{a}	112.68 ± 1.47^{a}	138.94 ± 1.02^{a}	105.38 ± 0.16^{a}	85.01 ± 0.26^{d}	119.60 ± 5.37^{b}	136.15 ± 1.00^{c}	31.03 ± 0.08^{b}	22.88 ± 1.69^{c}
	Intestinal	118.93 ± 0.30^{a}	113.57 ± 0.83^{a}	134.61 ± 1.53^{a}	104.44 ± 0.24^{a}	35.49 ± 0.38^{d}	124.39 ± 4.13^{a}	492.47 ± 1.09^{c}	58.50 ± 0.20^{a}	35.01 ± 1.24^{a}
BFME	*Oral*	96.22 ± 0.43^{b}	103.52 ± 3.13^{b}	98.31 ± 0.27^{c}	99.43 ± 0.27^{a}	353.75 ± 1.32^{b}	33.01 ± 1.71^{c}	212.47 ± 1.86^{c}	80.44 ± 0.23^{a}	28.42 ± 1.47^{b}
	Gastric	99.59 ± 0.22^{b}	107.96 ± 3.06^{b}	124.11 ± 0.48^{b}	99.01 ± 0.05^{a}	630.67 ± 2.02^{b}	20.06 ± 1.09^{c}	213.98 ± 2.69^{b}	56.22 ± 0.45^{a}	23.07 ± 0.92^{c}
	Intestinal	97.53 ± 0.11^{b}	103.90 ± 1.03^{b}	123.00 ± 0.28^{b}	99.38 ± 0.49^{a}	286.45 ± 1.67^{b}	43.53 ± 3.09^{c}	502.05 ± 1.74^{c}	41.19 ± 0.31^{b}	25.09 ± 0.92^{b}
BFAE	*Oral*	74.49 ± 0.77^{c}	105.36 ± 0.41^{b}	100.91 ± 0.88^{c}	99.94 ± 0.18^{a}	260.47 ± 3.67^{c}	130.32 ± 0.74^{a}	269.03 ± 2.31^{b}	82.96 ± 0.25^{a}	29.03 ± 1.42^{b}
	Gastric	102.64 ± 1.93^{a}	110.34 ± 1.15^{a}	116.97 ± 0.40^{b}	98.59 ± 0.27^{a}	492.11 ± 3.72^{c}	145.72 ± 2.79^{a}	244.10 ± 2.43^{b}	52.35 ± 0.05^{a}	29.34 ± 1.86^{a}
	Intestinal	103.83 ± 0.07^{b}	112.70 ± 0.33^{a}	115.26 ± 0.63^{b}	96.32 ± 0.76^{b}	425.15 ± 0.74^{a}	79.68 ± 0.87^{b}	686.71 ± 0.83^{b}	50.28 ± 0.11^{a}	25.17 ± 0.74^{b}

Values are expressed as mean of triplicate determination ($n = 3$) ± standard deviation. The mean values were statistically significant at $p < 0.05$ where a>b > c > d. BFPE- *B. fungosa* Petroleum ether extract; BFEA - *B. fungosa* Ethyl acetate extract; BFME - *B. fungosa* Methanolic extract; BFAE - *B. fungosa* Aqueous extract;

carbohydrate BA has been recorded by BFEA at the intestinal phase (35.49 %). The bioactive BFME showed a remarkable release of carbohydrates at the gastric phase to an extent of 630.67 % and a gradual reduction at the intestinal phase (286.45 %). The amino acids have witnessed a paramount release profile by BFPE with a BAI of 894.91 %, while the least amount of release was recorded by the gastric phase of BFEA (136.15 %). The BA of protein levels has been deemed to be highest in the gastric phase of aqueous extract (145.72 %), while the drastic decrease in the intestinal phase (79.68 %) has shown the metabolic fate of proteins in the alkaline pH environment. As far as phenolic compounds are concerned, the highest BA (above 80 %) has been recorded by BFME and BFAE at their oral phases. The lowest BA level has been shown by BFEA at its gastric phase (31.03 %). BFME has shown a gradual decrease in phenolic components, with a distinct degradation pattern, which indicates the easy absorption of phenolics present in the extract. Flavonoids, on the other hand, have shown the highest BA in the BFPE intestinal phase (35.28 %) while BFME has shown steady maintenance of the flavonoid BA level within the optimum range in each phase of digestion (23.07–28.42 %).

3.8. Metabolite analysis of bioactive extract by LC-qTOF-MS

The *B. fungosa* methanolic extract (BFME) was analysed using LC-qTOF-MS to identify the bioactive compounds. The mass-to-charge ratio (m/z) of the molecular and distinctive ions was utilised to determine the makeup of each peak. Fig. 1A represents the LC-qTOF-MS chromatogram of the bioactive compounds in BFME. As shown in Table 3, a total of 19 bioactive compounds were identified, and their pharmacological activities are reviewed from the NPASS (Natural Product Activity and Species Source) database. The NPASS database helps to acquire information on natural product and their bioactivity. It accounts for complete source, biological activity, and molecular target-based information, which can provide a faster route to the discovery of bioactive compounds in drug development and natural product research (Zhao et al., 2023). Using retention times, the mass spectra in literature data, and the UNIFI Waters library, each chromatogram peak was approximated. UNIFI Waters Library is a powerful tool for analysing mass spectrometric data. As such, it includes large databases for small molecules, metabolites, and peptides together with tools to aid in compound identification, structural elucidation, and quantification necessary for pharmaceutical research; as well as solutions aimed at the areas of both metabolomics (broad-scale discovery) and biomarker validation (Rosnack et al., 2016). Most of the identified compounds possess anti-inflammatory potential, especially Balanophotannin A, Ellagic acid, Gallic acid, Coumaric acid, and Amyrin, which were all reported already for their immense bioactivity and as constituents in many anti-inflammatory medications.

3.9. Validation and quantification of bioactives by HPLC

HPLC analysis revealed the quantitative presence of key bioactives such as Gallic acid, p-coumaric acid, trans-cinnamic acid, Tannic acid (associated with Balanophotannin A), β-sitosterol (associated with Daucosterol), Rutin, and quercetin (Fig. 1B). β-Sitosterol was found to be higher in quantity (30.250 mg/g), followed by large proportions of gallic acid (17.026 mg/g), ellagic acid (13.466 mg/g), and tannic acid (11.651 mg/g). The analysis has validated the confirmatory presence of the phytocompounds identified by LC-TOF-MS and has also quantified their bioactive components.

3.10. Identification of functional groups of the bioactive extract

The FTIR analysis (Fig. 2) has resulted in the observation of predominant alcohol and amine groups in the functional group and fingerprint regions, respectively. The broad wave at 3335.28 has been attributed to free alcohol groups with OH stretching vibrations. Prominent fingerprint region peaks were 1715.37, 1606.41, 1339.32, 1216.86, and 1024.98 $cm^{-1,}$ which corresponded to saturated aliphatic ketone groups, trisubstituted vinylene groups that occurred repeatedly, amines and acetals, primary and secondary free alcohols, respectively (Supplementary Table 4).

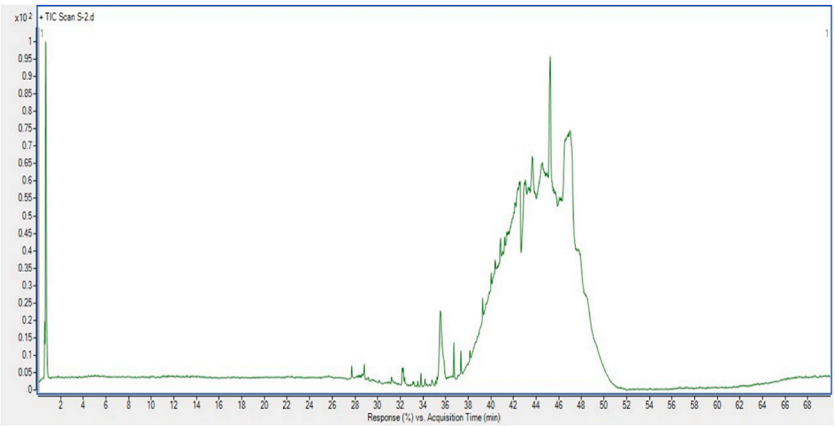

Fig. 1A. Metabolite analysis by Liquid Chromatography – Time of Flight – Mass Spectrometry (LC-TOF-MS).

Table 3
Metabolite analysis of BFME by LC-qTOF-MS analysis.

S. No	RT (min)	Component name	Chemical formula	Exact mass	Precursor mass	Height	Area	Error	Score	Pharmacological activity *(Adapted from NPASS)*
1.	40.685	Balanophotannin A	C_{34} H_{24} O_{21}	768.0747	769.0788	8049	20581	−8.24	17.38	Anti-inflammatory, Antioxidant, Immuno-moderant, Transcription factor NF kappa B inhibitor.
2.	0.561	Brevifolin	C_{12} H_8 O_6	248.0351	249.0431	3320	10338	12.12	26.4	Interleukin antagonist, TNF expression inhibitor, Anti-inflammatory, Non-steroidal anti-inflammatory agent.
3.	43.725	Daucosterol	C_{35} H_{60} O_6	576.4378	577.448	7622	26300	−2.03	54.88	Prostaglandin-E2 9-reductase inhibitor, Transcription factor NF kappa B stimulant, Interleukin 2 agonist, Anti-inflammatory.
4.	0.578	Ellagic acid	C_{14} H_6 O_8	302.0026	303.0099	3143	18011	−12.18	17.71	Anti-inflammatory, Interleukin 4 antagonist, TNF expression inhibitor, Lipoxygenase inhibitor.
5.	0.578	Gallic acid	C_7 H_6 O_5	170.021	171.0301	1974	3755	−3.3	48.95	TNF expression inhibitor, Anti-inflammatory, transcription factor NF kappa B stimulant, Interleukin 10 agonist.
6.	40.037	Lupeol	C_{30} H_{50} O	426.3871	427.3946	34543	119870	2.26	77.87	Caspase 3 stimulant, Transcription factor NF kappa B stimulant, Anti-inflammatory, Antioxidant.
7.	0.594	m-Coumaric acid	C_9 H_8 O_3	164.0467	165.0541	2319	7097	−3.99	76.03	TNF expression inhibitor, Anti-inflammatory, Antioxidant, Nitric oxide antagonist.
8.	47.846	Methyl coniferin	C_{17} H_{24} O_8	356.1377	357.1451	28535	281479	−26.44	51.54	Anti-inflammatory; Anti-cancer agent.
9.	0.594	p-Coumaric acid	C_9 H_8 O_3	164.0467	165.0541	2319	7097	−3.99	76.03	TNF expression inhibitor, Anti-inflammatory, Interleukin antagonist, Transcription factor NF kappa B inhibitor.
10.	38.076	p-Methoxycinnamic acid	C_{10} H_{10} O_3	178.0631	179.0697	1065	3733	0.48	75.15	Nitrite reductase (NO-forming) inhibitor, Free radical scavenger, Interleukin antagonist, Spasmolytic.
11.	32.195	trans Cinnamic acid	C_9 H_8 O_2	148.0518	149.0591	8553	36368	−4.24	83.97	Cytoprotectant, Anti-inflammatory, TNF expression inhibitor.
12.	40.037	β-Amyrin	C_{30} H_{50} O	426.3871	427.3946	34543	119870	2.26	77.87	Lipoxygenase and Cyclooxygenase inhibitor; Anti-cancer and Anti-inflammatory;
13.	42.296	β-Amyrin acetate	C_{32} H_{52} O_2	468.4114	469.4184	11767	69568	31.42	30.45	Anti-inflammatory; Anti-cancer agent; Anti-microbial agent;
14.	40.037	β-Amyron	C_{30} H_{48} O	424.3726	425.3799	110501	398685	4.98	37.73	Lipoxygenase and Cyclooxygenase inhibitor; Anti-cancer and Anti-inflammatory;
15.	44.655	beta-Amyrin palmitate	C_{46} H_{80} O_2	664.6121	665.6194	6769	41059	−5.61	31.18	Cyclooxygenase inhibitor; Anti-cancer agent.
16.	40.037	Taraxasterone	C_{30} H_{48} O	424.3726	425.3799	110501	398685	4.98	37.73	Anti-cancer agent; Anti-vascular inflammatory agent.
17.	38.143	Palmitic acid	C_{16} H_{32} O_2	256.2386	257.2459	9048	33851	−6.3	77.16	Nuclear factor erythroid 2-related factor 2 inhibitor; Peroxisome proliferator-activated receptor delta targeter;
18.	46.167	(6aR,6bS,8aR,12aS,14aR,14bS)-4,4,6a,6b,8a,11,11,14b-octamethyl-1,2,4a,5,6,7,8,9,10,12,12a,14a-dodecahydropicene-3,14-dione	C_{30} H_{46} O_2	438.3484	439.3579	5063	36808	−3.17	49.83	Anti-inflammatory; Anti-cancer agent;
19.	40.037	Isolactucerol	C_{30} H_{50} O	426.3871	427.3946	34543	119870	2.26	77.87	Anti-cancer agent; Anti-vascular inflammatory agent.

Ion Polarity – Positive; Adduct ions [M+H]+; RT- Retention Time; BFME - Balanophora fungosa methanolic extract; LC-TOF-MS - Liquid Chromatography – Time of Flight – Mass Spectrometry; NPASS-Natural Product Activity and Species Source database.

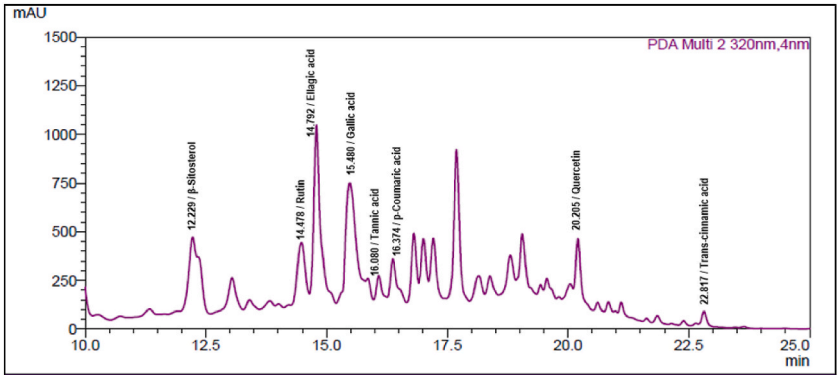

BFME Compounds	β-sitosterol	Rutin	Ellagic acid	Gallic acid	Tannic acid	p-Coumaric acid	Quercetin	Trans-Cinnamic acid
Quantity (mg/g)	30.250	8.320	13.466	17.026	11.651	5.414	4.526	1.296

Fig. 1B. Validation and quantification of identified BFME compounds by HPLC.

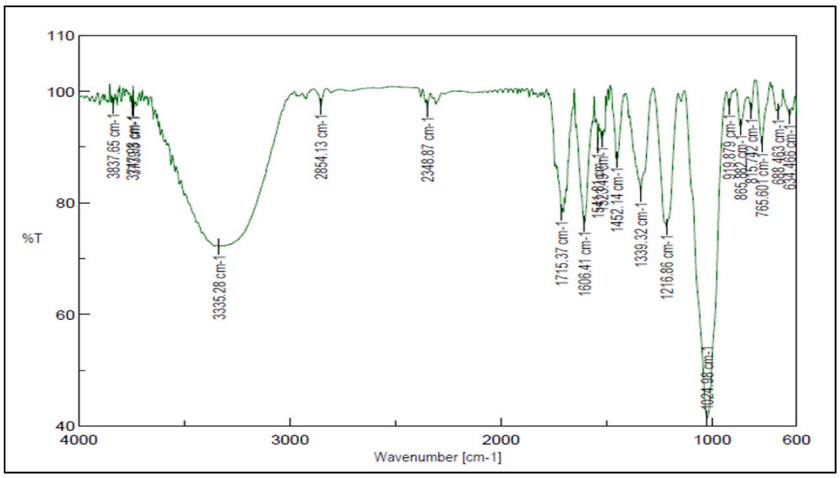

Fig. 2. Fourier Transform Infrared Spectral image of *Balanophora fungosa* Methanolic Extract (BFME).

3.11. Molecular docking of phytocompounds with inflammation proteins

Based on the results from the *in vitro* anti-inflammatory activity (Fig. 3; Table 4), the BFME was screened to be the most bioactive extract exhibiting anti-inflammatory activity. *B. fungosa m*ethanolic extract resulted in 19 small molecules from the LC-TOF-MS analysis, which were docked with inflammation-associated proteins to determine the interaction profile of lead compounds with the best dock scores.

1VKX (NF-kB complex) protein bound only with Balanophotannin A and produced a dockscore of −11.24 kcal/mol with a hydrogen bond of −4.404. The residues ASP185, 151, 153, LYS123, and ASN155 were responsible for the binding through hydrogen bonding in hydrophobic domains. Standard drugs diclofenac and aspirin depicted a dockscore of −3.659 and −3.021 kcal/mol, respectively, less than that of BFME compounds.

From the molecular docking results of 3GIO (TNF-alpha receptor), all 573 stereoisomers of 19 compounds were bound and showed potential binding energy. The compound Balanophotannin A produced the highest docking score of −12.81 kcal/mol with the H-bond of −5.63 by the strong interaction of LYS A:102, LYS B: 104, ASN A:99, TYR A: 94, ASN B:99, and TYR B:94 amino acids depicting hydrogen bonding and Pi cationic stacking. Compared to BFME compounds, diclofenac and aspirin showed a lower dock score of −4.548 and −2.874 kcal/mol, respectively.

From the molecular docking results of 1I1R (Interleukin 6 complex) protein, it is evident that Balanophotannin A produces a docking score of −10.75 kcal/mol with a hydrogen bond of −2.313, while diclofenac and aspirin were found to have lower docking scores of −5.245 and −4.875 kcal/mol. The residues ALA 44, ILE 46, HIS 48, and ARG 137 were found to be responsible for the binding through hydrogen bonding, Pi-Pi stacking, and salt bridges.

4OM7 (TLR-6 receptor) protein only interacts with 32 isomers of small molecules (ligands), among the results, p-Coumaric acid is

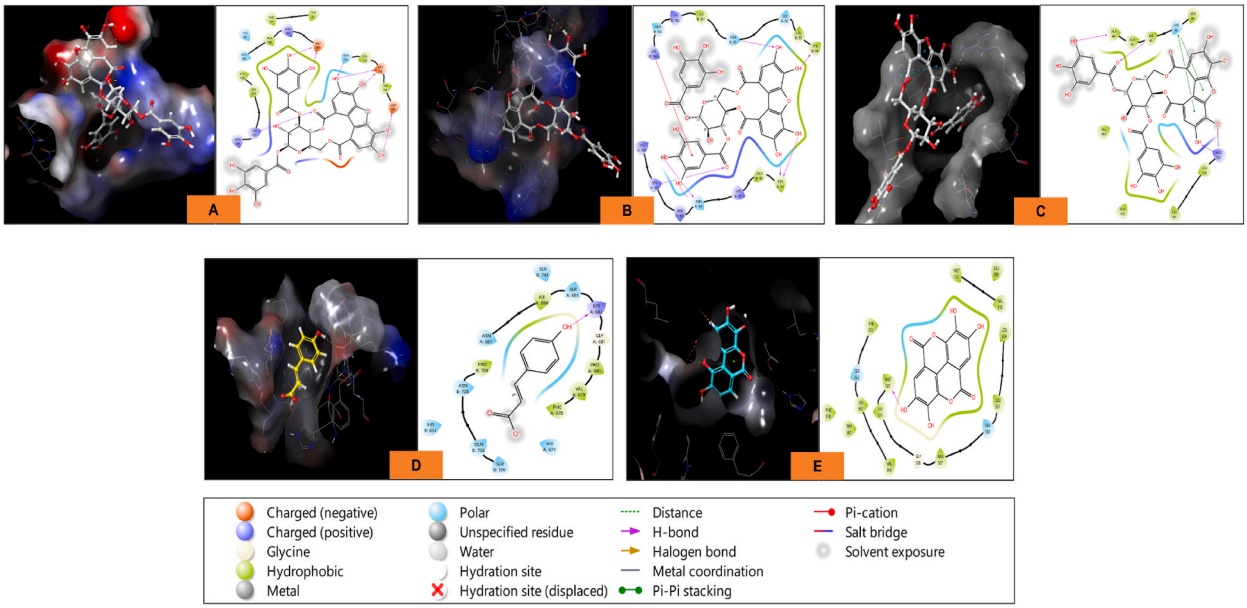

Fig. 3. Molecular Docking of *Balanophora fungosa* Methanolic Extract (BFME) compounds with **A:** NFkB protein; **B:** TNF-alpha receptor; **C:** IL6 receptor; **D:** TLR-6 receptor; **E:** COX-1 receptor.

the only compound that produced the binding energy of −4.17 kcal/mol with −1.198 H-bond, the rest of the small molecules (ligands) may exhibit the affinity below −4 kcal/mol. LYS A:682 residue of the protein directly interacted with the ligand through hydrogen bonding in hydrophobic polar domains. Notably, diclofenac and aspirin were found to have lower dock scores of −4.457 and −3.489 kcal/mol.

3KK6 (COX 1 receptor) protein docked with 11 stereoisomers among the 573, and there was no direct interaction found in the 2D interaction diagram. The compound ellagic acid potentially produces −6.9 kcal/mol of binding energy with MET 255 only through hydrogen bonding in hydrophobic polar domains with −1.92 H-Bond value. Fortunately, the dockscore was comparably appreciable with that of diclofenac (−8.05 kcal/mol) and aspirin (−5.465 kcal/mol).

The standard drugs (control), such as Diclofenac and Aspirin, showed lower dock scores (>-4 kcal/mol) than the BFME compounds, indicating the superiority of phytocompounds in targeting the inflammatory proteins. The docking profiles and interaction poses of standard compounds are tabulated and illustrated in Supplementary Table 5 and Supplementary Fig. 1, respectively.

3.12. Molecular dynamics simulation study

Molecular dynamics simulations of 100 ns were conducted to evaluate the stability and binding patterns between five phyto-compounds with inflammatory proteins. Protein–ligand contact profiling provides insights into the binding conformations, interaction dynamics, and structural integrity of the complexes under near-physiological conditions.

In the simulation of NFkB – Balanophotannin A complex, protein RMSD fluctuated within 2.1–2.9 Å after 12 ns, signifying a stable orientation (2.3 Å). RMSF plots showed higher fluctuations near the N-terminal region (>2.5 Å), while key interacting residues, including ASP185, GLN220, maintained their contacts with the ligand for over 70 % of the trajectory. The ligand formed stable H-bonds and hydrophobic contacts, especially through its sugar moieties and phenyl ring systems.

During the simulation of TNF alpha–Balanophotannin A complex protein, RMSD ranging between 1.6 and 2.5 Å an acceptable range, and ligand RMSD maintains a narrow window of 1.5–2.1 Å. The RMSF data revealed that regions between residues 110–145, corresponding to loop domains, showed moderate flexibility, while core residues such as ASN107, GLN110, and TYR112 remained stable and formed frequent hydrogen bonds (>65 % of the time). Hydrophobic interactions with residues like PHE74 and ILE109 further contributed to ligand anchoring.

The 100 ns molecular dynamics simulation of the Balanophotannin A–IL6 complex revealed stable protein-ligand interactions under physiological conditions (300 K, NPT ensemble). The protein RMSD stabilized around 2.2 Å, indicating a well-equilibrated structure with no significant conformational drift. The ligand RMSD (Lig fit Prot) fluctuated within 1.5–2.8 Å, suggesting the ligand remained stably bound in the protein's binding pocket throughout the simulation. The protein RMSF highlighted higher flexibility at the terminal residues and loop regions, while core residues involved in ligand binding remained rigid. The complex maintained 3–5 hydrogen bonds, 1–2 ionic interactions, and multiple hydrophobic contacts, with some interactions persisting for over 80 % of the trajectory. The secondary structure content remained stable, with 22.37 % α-helix and 27.46 % β-strand throughout. These results confirm that the Balanophotannin A exhibits high binding stability and favorable conformational accommodation within the IL6 binding site.

Table 4
Molecular Docking Profile of BFME lead compounds with inflammation proteins.

Protein	PubChem ID	Ligand	Dock score (kcal/mol)	H-bond	Lipophilicity	Electro-negativity value
NF-kB (1VKX)	11216477	Balanophotannin A	−11.24	−4.40	−1.99	−2
TNF-α (3GIO)	11216477	Balanophotannin A	−12.81	−5.63	−3.52	−1.81
	5742590	Daucosterol	−6.62	−2.79	−3.44	−0.61
	259846	Lupeol	−4.83	−0.7	−4.11	−0.15
	66654	Brevifolin	−4.68	−1.44	−2.28	−0.48
	405496034	beta-Amyrone	−4.45	−0.7	−3.41	−0.05
	637541	p-coumaric acid	−4.24	−1.54	−2.28	−0.56
	13915599	beta-Amyrin palmitate	−4.19	0	−4.7	−0.08
	71307372	(6aR,6bS,8aR,12aS,14aR,14bS)-4,4,6a,6b,8a,11,11,14b-octamethyl-1,2,4a,5,6,7,8,9,10,12,12a,14a-dodecahydropicene-3,14-dione	−4.18	−0.7	−3.03	−0.15
	370	Gallic acid	−4.07	−1.1	−1.91	−0.38
	115250	Isolactucerol	−4.06	−0.7	−3.22	−0.26
	250086235	Beta-Amyrin acetate	−3.98	−0.7	−2.96	−0.17
	637542	p-coumaric acid	−3.82	−1.23	−2.36	−0.35
	14485466	Taraxasterone	−3.68	0	−3.69	−0.02
	444539	Cinnamic Acid	−2.67	−0.35	−2.35	−0.32
	985	Palmitic Acid	−1.15	−1.06	−1.81	−1.66
IL-6 (1I1R)	11216477	Balanophotannin A	−10.75	−2.313	−3.47	−1.79
	5742590	Daucosterol	−4.97	−2.42	−2.19	−0.94
	637541	3-Hydroxycinnamic acid	−4.01	−1.29	−2.18	−0.44
	370	Gallic acid	−3.67	−2.18	−0.55	−0.82
	637542	p-coumaric acid	−3.61	−1.33	−1.89	−0.47
	13915599	beta-Amyrin palmitate	−3.37	−0.7	−3.38	−0.24
	250086235	Beta-Amyrin acetate	−2.93	−0.55	−2.48	−0.02
	115250	Isolactucerol	−2.84	−0.7	−2.47	−0.39
	259846	Lupeol	−2.64	−0.94	−1.57	−0.44
	444539	Cinnamic Acid	−2.56	−0.35	−1.97	−0.22
	71307372	(6aR,6bS,8aR,12aS,14aR,14bS)-4,4,6a,6b,8a,11,11,14b-octamethyl-1,2,4a,5,6,7,8,9,10,12,12a,14a-dodecahydropicene-3,14-dione	−2.38	−0.68	−1.78	−0.15
	66654	Brevifolin	−2.09	−0.96	−0.77	−0.34
	405496034	beta-Amyrone	−1.94	0	−2.24	−0.04
	14485466	Taraxasterone	−1.88	0	−1.95	−0.08
	985	Palmitic Acid	−0.86	−1.35	−2.45	−0.37

(*continued on next page*)

Table 4 (*continued*)

Protein	PubChem ID	Ligand	Dock score (kcal/mol)	H-bond	Lipophilicity	Electro-negativity value
TLR-6 (4OM7)	637542	p-coumaric acid	−4.17	−1.198	−1.83	−0.45
	637541	m-coumaric acid	−3.62	−1.64	−1.05	−0.52
	66654	Brevifolin	−3.38	−1.2	−0.47	−0.5
	250086235	Beta-Amyrinacetate	−2.69	−0.7	−1.98	−0.25
	259846	Lupeol	−2.38	−0.7	−1.73	−0.3
	115250	Isolactucerol	−2.04	0	−2.17	−0.04
	444539	Cinnamic Acid	−1.86	−0.46	−1.07	−0.02
	405496034	beta-Amyrone	−1.68	0	−1.97	0.04
	13915599	beta-Amyrin palmitate	−1.41	0	−3.04	−0.03
	14485466	Taraxasterone	−0.99	0	−1.58	−0.01
COX-1 (3KK6)	5281855	Ellagic acid	−6.9	−1.92	−5.46	0.05
	370	Gallic acid	−6.58	−2.25	−2.7	−0.35
	66654	Brevifolin	−5.84	−1.09	−3.73	−0.39
	637542	p-coumaric acid	−5.8	−1.59	−2.89	−0.37
	985	Palmitic Acid	−5.34	0	−4.45	−0.07
	637541	p-coumaric acid	−5.02	−0.44	−3.26	−0.06
	444539	Cinnamic Acid	−4.93	−0.16	−3.28	−0.14
	13915599	beta-Amyrin palmitate	−4.32	0	−5.48	0.02
	115250	Isolactucerol	−3.77	−0.7	−3.14	−0.14

BFME - B. fungosa methanolic extract.

In the COX1 receptor – Ellagic acid complex, both protein and ligand RMSD curves demonstrated rapid stabilization. The protein RMSD plateaued at ~2.3 Å after 10 ns, and the ligand RMSD remained stable between 1.8 and 2.2 Å, denoting minimal drift from the binding pocket. RMSF analysis showed that catalytic residues involved in ligand interactions, such as ARG110, TYR59, and GLU146, fluctuated below 1.5 Å. These residues formed stable hydrogen bonds and ionic bridges for over 60 % of the simulation time, reinforcing the binding stability of the complex. The TLR 6 6-p-Coumaric acid complex observed consistent protein RMSD between 1.7 and 2.4 Å and ligand RMSD within 1.5–2.3 Å over the duration of 100 ns. The RMSF analysis showed typical flexibility in terminal regions and loops, whereas interacting residues such as TYR385, SER530, and HIS90 showed minimal fluctuations (<1.8 Å). These residues consistently engaged in hydrogen bonding and π-π interactions, maintaining occupancy levels above 75 %. The ligand also exhibited minimal internal torsional fluctuations, reflecting a well-fitted conformation within the binding groove.

Overall, the RMSD and RMSF profiles across all complexes indicated well-equilibrated systems with high structural integrity. The

Table 5
Analysis of pharmacokinetic properties of BFME lead compounds by ADMET analysis.

ADMET Properties	qIKPROP Standard Value	Balanophotannin A (PubChem ID: 11216477)	Ellagic Acid (PubChem ID: 5281855)	p- Coumaric Acid (PubChem ID: 637542)
#stars	0–5	9	1	0
#amine	0–1	0	0	0
#amidine	0	0	0	0
#acid	0–1	0	0	1
#amide	0–1	0	0	0
#rotor	0–15	15	4	4
#rtvFG	0–2	5	2	1
CNS	+2 is active; −2 is inactive	−2	−2	−2
mol_MW	130.0–750.0	768.551	302.197	164.16
dipole	1.0–12.5	4.858	0	5.75
SASA	300.0–1000.0	974.107	455.912	377.068
FOSA	0–750.0	81.484	0	23.541
FISA	7.0–330.0	636.267	326.676	168.945
PISA	0.0–450.0	256.356	129.236	184.582
WPSA	0.0–175.0	0	0	0
volume	500.0–1000.0	1867.444	775.414	585.987
donorHB	0.0–6.0	11	4	2
accptHB	2.0–20.0	19.4	8	2.75
dip^2/V	0.0–0.13	0.0126391	0	0.0564223
ACxDN^0.5/SA	0.0–0.05	0.0660528	0.0350945	0.010314
glob	0.75–0.95	0.7528759	0.8953093	0.8981274
QPpolrz	13.0–70.0	61.398	23.544	16.492
QPlogPC16	4.0–18.0	24.639	9.665	6.543
QPlogPoct	8.0–35.0	49.39	18.473	10.324
QPlogPw	4.0–45.0	40.046	16.773	7.787
QPlogPo/w	2.0–6.5	−2.442	−1.294	1.425
QPlogS	6.5–0.5	−4.262	−1.918	−1.648
CIQPlogS	6.5–0.5	−7.653	−3.214	−1.812
QPlogHERG	Concern below 5	−6.753	−3.842	−2.253
QPPCaco	<25 poor; >500 great	0.009	7.907	62.719
QPlogBB	3.0–1.2	−7.824	−2.395	−1.074
QPPMDCK	<25 poor; >500 great	0.002	2.645	31.544
QPlogKp	−8.0 to −1.0	−10.903	−6.701	−3.599
IP(eV)	7.9–10.5	8.741	9.28	9.262
EA(eV)	0.9–1.7	0.997	1.383	0.846
#metab	1–8	12	4	1
QPlogKhsa	−1.5 - 1.5	−0.955	−0.658	−0.67
Human Oral Absorption	–	1	2	3
% Human Oral Absorption	>80 % high; <25 % poor	0	35.438	67.46
SAfluorine	0.0–100.0	0	0	0
SAamideO	0.0–35.0	0	0	0
PSA	7.0–200.0	373.596	165.2	73.888
#NandO	2–15	21	8	3
Rule Of Five	Max is 4	3	0	0
Rule Of Three	Max is 3	2	1	0
#ringatoms	–	36	16	6
#in34	–	0	0	0
#in56	–	31	16	6
#noncon	–	6	0	0
#nonHatm	–	55	22	12

BFME - Balanophora fungosa methanolic extract; ADMET- Absorption, Distribution, Excretion, Metabolism and Toxicity.

duration and stability of protein–ligand contacts—especially hydrogen bonds and hydrophobic interactions—were maintained over >60–80 % of the simulation time, strongly supporting the robustness and potential therapeutic relevance of the studied phytocompounds. These MD simulations validate the docking poses and highlight stable ligand accommodation within the catalytic sites of each target.

3.13. Binding free energy calculation

Binding free energy calculations derived from Equation (4) resulted in the following ranking among the simulated complexes: NFkB complex (−147.55 kcal/mol) > IL 6 complex (−123.02 kcal/mol) > TNF α complex (−112.15 kcal/mol) > COX1 complex (−21.69 kcal/mol) > TLR 6 complex (−18.41 kcal/mol). A predominant hydrogen and hydrophobic bonding domains in the bound complexes were found to be responsible, as observed from the MMGBSA analysis.

3.14. Assessment of pharmacokinetic properties of bioactive lead compounds

Balanophotannin A, ellagic acid, and p-coumaric acid of the methanolic extract of *B. fungosa* were subjected to pharmacokinetic properties (Table 5) by employing the QikProp module in Schrödinger Suite for virtual prediction of drug-likeness over various ADMET parameters. Of all the compounds studied, the pharmacokinetic profile of Balanophotannin A is impressive, which means that this represents the most promising drug candidate among these compounds compared to ellagic acid and p-coumaric acid.

One of the main factors that characterizes the similarity of a drug is its molecular weight (mol_MW). The standard range for this descriptor falls between 130.0 and 750.0 g/mol. Based on this, the molecular weight for Balanophotannin A is 768.551 g/mol, which is slightly above the recommended upper limit, while ellagic acid and p-coumaric acid have molecular weights of 302.197 and 164.16 g/mol, respectively, each well within the limit. Therefore, Balanophotannin A may be regarded as larger and hence might pose problems in permeability and absorption. Also, water solubility, as calculated by QPlogS and CIQPlogS, is another important parameter for oral administration. The QPlogS of Balanophotannin A is −4.262, reflecting its poor solubility compared with the relatively better solubility profiles of ellagic acid and p-coumaric acid, with QPlogS values of −1.918 and −1.648, respectively.

Lipophilicity, defined as the partition coefficient octanol/water, QPlogPo/w, is one of the important determinants of drug absorption. QPlogPo/w of −2.442 for Balanophotannin A is hereby considered to show low lipophilicity and thus may imply poor permeation through the lipid membranes. On the other hand, p-coumaric acid had a QPlogPo/w of 1.425, showing better permeability through the lipid membranes, hence the better absorption of drugs. Polar surface area values also reflect permeability. Balanophotannin A has a polar surface area value of 373.596 $Å^2$ against ellagic acid at 165.2 $Å^2$ and p-coumaric acid at 73.888 $Å^2$. A higher PSA tends to reduce membrane permeability, including oral absorption, and thus may be a weakness for Balanophotannin A.

The central nervous system (CNS) activity and the blood-brain barrier permeation are very important aspects for drugs that may be used in combating neurological disorders. The three compounds under consideration have a CNS of −2, which represents inactivity. However, Blood-Brain barrier (BBB) permeability is highly variable, with QPlogBB ranging from a very low −7.824 for Balanophotannin A, indicating negligible BBB penetration, to −2.395 and −1.074 for ellagic acid and p-coumaric acid, respectively, which are much better potential drug candidates.

The percentage of human oral absorption for Balanophotannin A is forecasted at 0 %, which is considerably less than of ellagic acid and p-coumaric acid at 35.438 % and 67.46 %, respectively. This poor absorption, coupled with its poor permeability of 0.009 nm/s and 0.002 nm/s from the calculated QPPCaco and QPPMDCK values, respectively, indicates high challenges in oral delivery for the Balanophotannin A. On the other hand, p-coumaric acid presents favorable values in both permeability metrics −62.719 cm/s and 31.544 cm/s, respectively-suggesting it may have better oral bioavailability.

Hydrogen bonding capabilities are critical features in drug interaction with biological targets. Meanwhile, Balanophotannin A has a high number of hydrogen bond donors and acceptors at 11 and 19.4, compared to ellagic acid with 4 donors and 8 acceptors and p-coumaric acid with 2 donors and 2.75 acceptors. While these interactions can enhance binding affinity, it is worth noting that extensive hydrogen bonding can reduce membrane permeability, a possible limitation with Balanophotannin A. Moreover, the number of metabolic reactions (#metab) for Balanophotannin A was 12, representing a higher degree of metabolic instability compared to ellagic acid (4) and p-coumaric acid (1). This would consequently suggest that active metabolism may occur for Balanophotannin A, reducing its half-life and therapeutic effectiveness.

The toxicity of the drug is the main issue during the pharmaceutical development process. In this respect, the QPlogHERG value of Balanophotannin A is −6.753, meaning that the drug can cause some cardiotoxicity problems through inhibition of the hERG potassium channel, a frequently occurring problem in some drug candidates of drugs. On the other side, ellagic acid and p-coumaric acid have QPlogHERG values of −3.842 and −2.253, respectively, indicating drugs presenting minimal risks of showing cardiotoxicity. Besides this, the follow-up of Lipinski's rule of five and of the rule of three also characterizes the complexity of Balanophotannin A. It meets three out of four criteria of Lipinski's rule and two out of three criteria of the rule of three, while ellagic acid and p-coumaric acid meet those rules more comfortably.

The molecular weight, solubility, and permeability of Balanophotannin A indicate certain weaknesses regarding bioavailability and drug likeness. On the other hand, it possesses some characteristic hydrogen-bonding potential and probable interaction profile that could be useful in specific therapeutic contexts. However, poor oral absorption, low BBB permeability, and possible toxicity are some of the issues that have to be addressed to improve its drug-likeness profile in comparison with the other two.

3.15. *In vivo anti-inflammatory activity*

As analysed by the croton oil-induced ear oedema assay (Fig. 4), locally administered *B. fungosa* methanolic extract revealed dose-dependent inhibitory effects in mouse inflammation. The untreated control was 26.32 g for the mean wet weight of the oedema, while

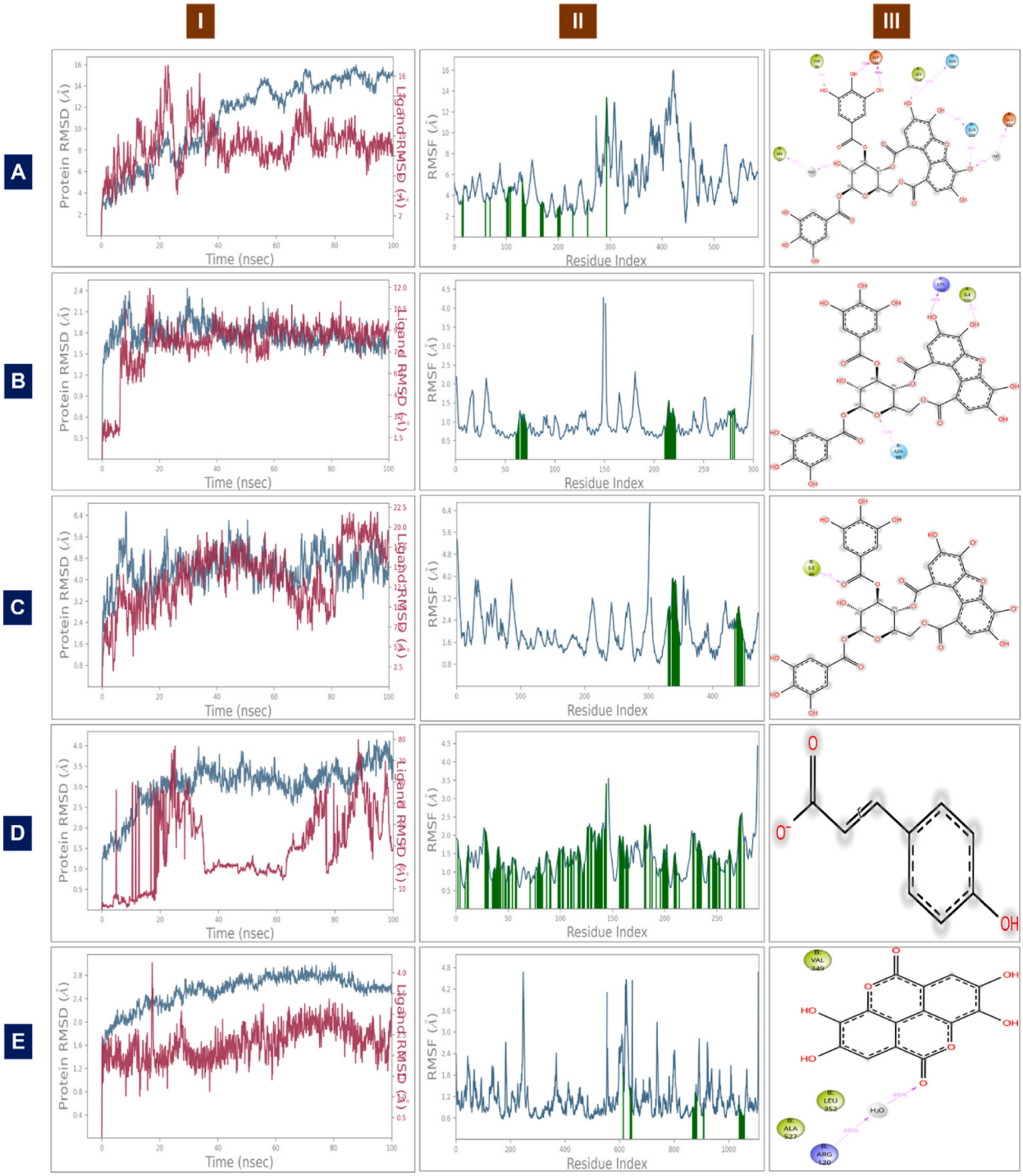

Fig. 4. Molecular Dynamics simulation analysis; **I-** Protein Ligand RMSD; **II-** Protein RMSF; **III-** Ligand Protein contacts; **A:** NFkB-Balanophotannin A complex; **B:** TNF-alpha receptor – Balanophotannin A complex; **C:** IL6 receptor- Balanophotannin A complex; **D:** TLR-6 receptor -p-Coumaric acid complex; **E:** COX-1 receptor-Ellagic acid complex.

croton oil treatment alone for the negative control registered a remarkable increase to 36.12 g of wet weight, ensuring the success of induction. Treatment with the standard anti-inflammatory drug Diclofenac also markedly cut down the oedema by 58.82 %, which vindicated the model's sensitivity. Attributing to the efficacy of bioactive compounds, *B. fungosa* extract at variable concentrations showed augmenting efficacy: the low concentration (50 mg/kg) decreased the oedema to 64.79 %, mid concentration (100 mg/kg) to 70.70 %, and high concentration (200 mg/kg) to 85.35 %, which was significant reduction as the untreated control retained 92.68 % unreduced oedema and the appreciably better than Diclofenac (see Fig. 5).

4. Discussion

In the present study, the potential of *Balanophora fungosa* extracts to act as an anti-inflammatory agent was analysed. The extracts were screened on the basis of their antioxidant properties as they provide valuable insights on the basis of inflammation cascades and are deeply correlated with pathways that govern inflammation in the human body (Adebayo et al., 2015).

The hot percolation method employed for the extraction of phytocompounds from powdered aerial parts of *B. fungosa* has yielded a high amount of extract with polar solvents, i.e., methanol and water, which depicts the presence of more polar compounds in *B. fungosa.* Hot percolation is a useful technique solicited by the Soxhlet apparatus to extract many thermo-stable phytocompounds, which can exert many physiological roles in an exothermic environment (Thilakarathna et al., 2023).

In the quantification of primary metabolites, an ample number of proteins were observed. This may be the reason for its fodder properties to musky rat kangaroos and other vertebrates, as reported previously (Pierce and Ogle, 2017). As far as secondary metabolites are concerned, *B. fungosa,* being a root parasite, can withstand stressful environments through allelopathic effects and its secretions. This has a deep connection with the number of secondary metabolites being produced by the plant as a mechanism to deter herbivory or competition (Chen et al., 2023). Hence, it can be affirmed that high levels of phenolic, flavonoid, and tannin compounds are present in the plant. Ethyl acetate, being the highlighted solvent for the extraction of these secondary metabolites, has proved its efficacy in extracting these secondary metabolites, due to its selectivity and ability to dissolve both lipophilic and hydrophilic compounds (Raina-Fulton and Mohamad, 2018).

From the results of the bioactivity profile analysis of *B. fungosa* extracts, it is evident that both methanol and ethyl acetate extracts have rendered equivalent antioxidant activity due to their proportionate composition of phenolics and flavonoids. Numerous plant species have already been studied in the past to determine how much their overall phenolic content contributes to their potential as antioxidants (Peron et al., 2024). More frequently, our cells react to polyphenols by directly interacting with signal-transduction receptors or enzymes, which may change the redox status of the cell and cause a number of redox-dependent processes (Moskaug et al., 2005).

The presence of more phenolics in the aerial sections of *B. fungosa* is a solid indicator of its enhanced antioxidant ability. Increased polymerization of the polyphenolic components already present in *B. fungosa* extracts may be the cause of the extracts' higher tannin content (Supplementary Table 2). Recent research has demonstrated that phenolics with a high molecular weight, such as tannins,

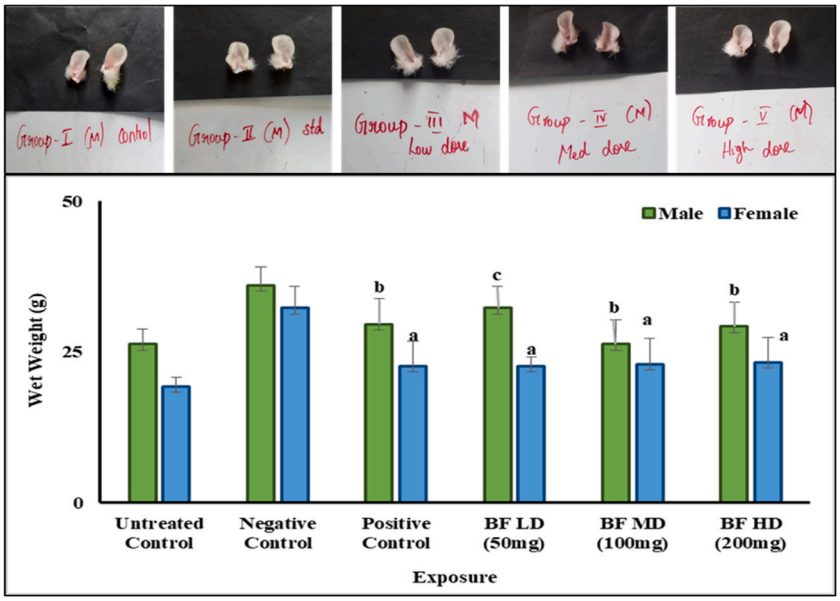

Fig. 5. Wet weight of ear biopsies from Croton oil induced ear oedema analysis Values are expressed as mean of triplicate determination (n = 6 independent biological mouse ears/group) and are considered significant when $p > 0.05$ and $^{a>b>c.}$ Negative control – Treated with croton oil only; Positive control – treated with Croton oil and Diclofenac (100 mg); BF LD- *B. fungosa* methanolic extract low dose; BF MD- *B. fungosa* methanolic extract mid dose; BF HD- *B. fungosa* methanolic extract high dose.

have a higher capacity to scavenge free radicals. The ability of *B. fungosa's* extracts to scavenge free radicals may also be enhanced by their tannin concentration. Flavonoids are also a broad and important class of natural phenolics. These compounds exhibit a wide range of chemical and biological activity. Flavonoids have been proven *in vitro* and in animal experiments to have anti-inflammatory, antioxidant, antiviral, antiallergenic, antithrombotic, hepatoprotective, and anticancer properties (Mariadoss et al., 2023). Furthermore, flavonoids have been discovered to meet the majority of the criteria for antioxidants: flavonoids block the enzymes involved in superoxide radical generation (Hu et al., 2023). As a result, quantifying the flavonoid concentration of plant components is critical since it can be linked to the plant's radical scavenging capacity. Since *B. fungosa* has significant flavonoid content in the aerial region (Supplementary Table 2), it might be expected that it can have a higher free radical scavenging activity.

The DPPH assay is valid and highly regarded for quantifying samples with hydrophilic or lipophilic antioxidants. In this test, a molecule or antioxidant with weak A-H bonds will discolour the molecule as a result of a reaction with the stable free radical DPPH• (λ_{max} = 517 nm). The method can be used to measure samples that include hydrophilic or lipophilic antioxidants (Wisetkomolmat et al., 2023). Although the DPPH radical scavenging activities of the different plant extracts seemed to be ordinary, it is not guaranteed that the plant has no potential for radical scavenging activities. The ability of different *B. fungosa* extracts to donate hydrogen and transfer electrons would be impacted by the type of phenolics and their antiradical scavenging activities. It has also been discovered that antioxidants that respond swiftly with peroxyl radicals may also react slowly with DPPH radicals (Hassan et al., 2023). We may thus conclude that *B. fungosa* might be able to combat DPPH with the increased presence of greater molecular weight polyphenolic antioxidant compounds and attribute its similarity to *B. laxiflora* (She et al., 2009) (Supplementary Table 2).

Given that the phosphomolybdenum test is straightforward and independent of other standard antioxidant assays used to quantify vitamins, it was decided to expand the usage of this method to plant extracts (Kotha et al., 2022). Additionally, it is a quantitative one since the amount of ascorbic acid equivalents is used to express antioxidant activity. As a result, the overall antioxidant capacity of *B. fungosa* extracts can be associated with the fact that they have free radical scavenging abilities comparable to those of ascorbic acid, a naturally occurring antioxidant.

Superoxide radicals are known to be incredibly harmful to cellular components since they are a precursor to additional reactive oxygen species. Numerous biological processes result in the production of superoxide radical, an extremely dangerous species. Although superoxide radical anions cannot directly induce lipid oxidation, they are powerful progenitors of highly reactive species such as the hydroxyl radical. Researching ways to scavenge this radical is therefore essential (Akbari et al., 2022). *B. fungosa* can be utilised to counteract the negative effects of hydrogen peroxide on the body since it demonstrated a significant proportion of scavenging activity.

In the FRAP test, excess Fe (III) is employed, and the rate-limiting factor of Fe (II)-TPTZ (2,4,6-Tris(2-pyridyl)-s-triazine), colour formation was used to do the FRAP assay, as it is the reducing ability of the antioxidant chemicals in the plant sample. This reduction can be because of the ability of iron targeting phenolics of BRME to reduce the ferric complex to ferrous ions (Lu et al., 2022).

One of the main instances of oxidative damage in biological systems is the peroxidation of cellular membranes brought on by ROS. It is thought that because erythrocyte cell membranes contain a significant amount of polyunsaturated fatty acids, they are a suitable model for studying lipid peroxidation. ROS produced by hydrogen peroxide or radicals produced directly during cellular metabolism cause membrane damage and haemoglobin leakage by oxidizing the lipids in cell membranes (Karim et al., 2020).

Based on this bioactivity profile analysis, BFME and BFEA were screened to further test for anti-inflammatory potential. Various studies were conducted on the goat erythrocyte membrane to validate the function of *B. fungosa* in stabilizing membranes. Numerous diseases are brought on by the release of lysosomal enzymes during inflammation. Since the components of RBC membranes are similar to those of lysosomal membranes, the anti-inflammatory efficacy of medications and plant extracts was evaluated by preventing hypotonicity-induced RBC membrane lysis. The outcomes showed that methanol extracts shield the erythrocyte membrane against lysis brought on by hypotonic conditions. The action was similar to that of Diclofenac. Other biomolecules can maintain the erythrocyte membrane and keep protein membranes from becoming denatured, whereas phenolics, flavonoids, tannins, and saponins can bind cations (Kalaiselvi and Vidhya, 2015). Therefore, the strong polyphenolic substances included in BFME, such as phenolic, tannin, and flavonoid compounds (Supplementary Table 2), may be the cause of their anti-denaturation properties and their capacity to stabilize the lysosome membrane by scavenging and inhibiting ROS and lipid peroxidation, respectively (Martínez et al., 2021). Previous reports on anti-inflammatory activity figure out that isolariciresinol, an isolated compound of *B. fungosa* subsp. *indica*, exhibited an anti-inflammatory activity of 56.02 % at 100 μg/mL, while the other compounds showed an inhibition range of 13.7–45.4 % (Tung et al., 2021).

Many different and numerous plant-derived substances have been found to obstruct the production of 5-LOX products, which exert significant anti-inflammatory activities. Leukotriene (LT) production is started by the 5-lipoxygenase (5-LOX)-mediated conversion of free arachidonic acid to LTA4. This is followed by the transformation of LTA4 into LTB4, cysteinyl-LTs C4, D4, and E4. Numerous inflammatory disorders, such as rheumatoid arthritis, cancer, osteoporosis, allergic rhinitis, inflammatory bowel disease and skin problems, bronchial asthma, and cardiovascular diseases associated with lung transplants, in which 5-LOX has significant pathophysiology roles. Blocking LT receptors, which serve as a channel for LT intervention, or pharmacologically and genetically disrupting the 5-LOX pathway may be useful as a treatment for inflammatory disorders (Piesche et al., 2020). Hence, as observed in the assay, BFME has proved to have high inhibition efficacy to 5-LOX (Supplementary Table 3) and thereby can be used as a candidate for anti-inflammatory drug development. Therefore, the metabolomic data of the BFME were mined to ascertain the responsible phytocompounds elucidating the anti-inflammatory activity.

The bio-accessibility (BA) of phytochemicals from petroleum ether (BFPE) and ethyl acetate (BFEA) extracts varies during *in vitro* digestion, which can be ascribed to their vulnerability to pH and temperature changes. Low-polar chemicals in these extracts may have a variety of effects against free radicals depending on their conjugates and interactions with reactive oxygen and nitrogen species (Seke

et al., 2022). The bioaccessibility of these compounds can be modified by digesting circumstances, such as pH changes, which might affect the release and availability of bioactive components (Melo et al., 2020). Furthermore, the bioaccessibility of plant extract components is influenced by their digestive stability and interactions with the gastrointestinal environment. Studies have demonstrated that the matrix effect and polymeric phenolic fraction present in extracts have been shown in studies to alter antioxidant bioaccessibility (Nieto et al., 2023). Furthermore, the digestive process might alter the bioaccessibility of phenolic compounds, resulting in structural alterations that may impair their bioavailability (Melo et al., 2020). Also, complex food matrix interactions can influence compound bioaccessibility during digestion, affecting bioactive component release and availability (Honaiser et al., 2022). The vulnerability of chemicals to pH changes during digestion can influence their bioaccessibility rates, as demonstrated by Cy-3-Sa and Cy-3-G during *in vitro* gastrointestinal digestion (Seke et al., 2022). These findings show the need to take pH and temperature into account when determining the bio-accessibility of chemicals in plant extracts during digestive processes.

Bio-accessibility index BAI above 100 % indicates the complexity of the biomolecules and the structural/conformational changes that they undergo during the digestion procedures when simulated *in vitro* (Andrade et al., 2022). The higher variation of BA of carbohydrates may be attributed to the influence of pH in the breakdown and release of carbohydrates from their complexes into the digestion matrix at the intestinal phase. As the intestinal phase is the major site for carbohydrate assimilation, the 3-fold gradual reduction in BA of BFME shows the level of bio-accessible carbohydrates in the intestinal phase and the influence of carbohydrate metabolizing enzymes and conditional alkaline pH (Durairajan et al., 2024). High release of amino acid levels depicts the high bioavailability of free amino acids in the extracts after *in vitro* digestion (Xia et al., 2017). Proteins, being pH and polarity-sensitive compounds, have eluted well in the aqueous extract. The low BA level at the intestinal phase of BFAE signifies the rate of absorption in the gastric phase due to the activity of pepsin and a bioavailable fraction of proteins at the preceding intestinal phase (Silva et al., 2021). Also, gradual absorption of phenolics, along each phase of digestion, highlights the significance of the crude extract in drug delivery through the GI tract in an easy manner (Schulz et al., 2017). Compared to the other phytoconstituents (carbohydrates, proteins, amino acids, and phenolics), the BA of flavonoids is relatively very low, showcasing the predominance of dietary bioactives and presence of therapeutic phytocomponents in permissible and requisite amounts in *B. fungosa* extracts. This attribution is in concordance with the relatively low bio-accessibility of flavonoids in plant extracts, which greatly depends on extraction techniques and treatment environment in *in vitro* digestion models (Bouayed et al., 2011). Hence, from the BAI analysis, it has been confirmed that the *B. fungosa* extracts exhibit a very competent profile when supplemented as food substrates with therapeutic efficacies that are enhanced during digestion events in the GI tract.

Metabolomics is focused on the thorough and quantitative examination of a diverse range of metabolites in biological specimens (Yao et al., 2022). The well-established technique of LC-MS in drug metabolite analysis (metabolomics) is currently being expanded to endogenous metabolite research. Its key benefits encompass a broad dynamic range, consistent quantitative analysis, and the capacity to assess biofluids with incredibly complex molecular compositions. The objectives of advancing LC-MS for metabolomics include gaining insights into fundamental biochemistry, identifying biomarkers, and characterizing the structure of metabolites that are crucial to physiological processes (Keen et al., 2022). Herein, the 19 compounds identified in the *B. fungosa* methanolic extract by LC-TOF-MS analysis possess remarkable pharmacological activity that are signified in Table 3 and are consistent with the exuberant anti-inflammatory activity observed *in vitro*.

Current advances in chiral HPLC have centered on high-throughput separations of biologically active chiral chemicals, especially of importance for pharmaceutical uses (De Luca et al., 2024). HPLC in conjunction with UV/Vis and mass spectrometry is routinely used to analyze phenolic compounds and flavonoids, which show potential health benefits (Côté et al., 2010). Online integration of biochemical detection assays with HPLC is a novel high-resolution screening method for the identification of bioactive molecules in plant extracts, devoid of the pitfalls of conventional bio-assay guided fractionation techniques. These online HPLC-biochemical detection assays consist of enzyme-based, receptor-based, and antioxidant assays (Malherbe et al., 2012).

Herein, from the current analyses, many bioactive compounds have been identified and are known for their pharmacological uses. β-sitosterol pre-treatment suppressed neutrophil recruitment and injury, reflecting a strong anti-inflammatory activity (Zhang et al., 2023); Rutin reduces inducible nitric oxide synthase (iNOS) gene and protein levels and enhances IκB gene expression in LPS-stimulated RAW 264.7 cells. In addition, rutin suppresses the expression of TLR4, MyD88, TRAF6, and p65 and blocks their phosphorylation, suggesting its modulatory effect on the TLR4-MyD88-TRAF6-NF-κB signaling pathway (Tian et al., 2021); Ellagic acid modulates inflammatory signals and cytokines (IL-1β, IL-6, TNFα, etc.) to display a positive inflammation effect. It also possesses a potent therapeutic action on diseases like diabetes, cancer, and depression that are associated with inflammation (Zhang, 2023); Gallic acid suppresses LDH release and pyroptosis in LPS-, ATP-, nigericin-, or MSU crystal-stimulated macrophages. It is also found to inhibit NLRP3 inflammasome activation through NLRP3-NEK7 interaction inhibition and ASC oligomerization, suppressing caspase-1 activation and IL-1β secretion. Gallic acid increases Nrf2 signaling, lowering mitochondrial ROS generation, and inhibits MSU-induced swelling of the joints and inflammatory cytokines in mice (Lin et al., 2020); Tannic acid is a major gastroprotective and anti-inflammatory compound that is known to decrease levels of TNF-α, IL-1β, and IL-6 (de Veras et al., 2021); Likewise, p-Coumaric acid (PCA) is known to lower oxidative stress by enhancing SOD and GSH contents and lowering levels of MDA. PCA exhibited anti-inflammatory actions by reducing levels of TNF-α and IL-6. PCA inhibited neuronal apoptosis by reducing caspase-3 and c-Jun levels, and decreased neuronal loss and histopathological abnormalities in the hippocampus (Daroi et al., 2022). Quercetin is a commonly ingested flavonoid and has strong anti-inflammatory action. It exerts its effects through interfering with inflammatory processes, such as blocking the NF-κB signaling pathway and lowering cyclooxygenase-2 levels. Notwithstanding its unfavorable bioavailability caused by extensive metabolism, quercetin efficiently regulates inflammation and immune response (Granado-Serrano et al., 2012; C. Nweze et al., 2022); trans-cinnamic acid regulates the decrease in inflammation by suppressing TNF-α, IL-6, and MPO activities as well as the expression of inflammatory cytokines and TLR-4 (Rezaei et al., 2024); A clear image of the metabolic makeup of

plant parts at a specific moment can be obtained using the physicochemical analytical method, Fourier transform infrared spectroscopy. By looking at the IR spectra, it is feasible to spot even small changes in the primary and secondary metabolites. FTIR can be used to determine the structure of unknown compositions and the intensity of absorption spectra linked to molecular composition or the presence of specific chemical functional groups. For many years, FTIR has been used to identify the complex structures of plant secondary metabolites as well as to characterise bacterial, fungal, and plant species (Thummajitsakul et al., 2020). Herein, the predominance of alcohol groups represents the extensive hydrogen bonding in the complex composition of phytocompounds of *B. fungosa*. Also, the repeated alcohol stretching, deformation, and rocking vibrations show the intense derivation of phytocompounds being substituted in their alkyl parts and side chains. Further, the distribution of vinylenes and vinyl ethers depicts the intensity of saturation observed in the carbonyl compounds of *B. fungosa*.

Numerous naturally occurring substances included in medicinal plants, including alkaloids, saponins, terpenoids, and flavonoids, have demonstrated anti-inflammatory properties both *in vitro* and *in vivo*. Many natural compounds have molecular targets and mechanisms of action that need to be investigated in order to establish a structure-activity relationship. Using molecular docking studies, one may look at how these organic compounds interact with various anti-inflammatory molecular targets. Furthermore, the structure-activity relationship can be exploited to create new natural chemicals with increased anti-inflammatory action.

NF-kB family transcription factors in eukaryotes regulate immune system gene expression. NFKB-inducing kinase (NIK) stimulates transcription, cytokine-induced signaling pathways, angiogenesis, and inflammation, controlling immune system genes. NIK is highly expressed in tumour endothelial cells and inflamed synovial tissues of rheumatoid arthritis (Herowati and Widodo, 2017). Balanophotannin A has demonstrated encouraging docking findings with the NF-kB complex, which are on par with the actions of common medications like diclofenac and aspirin. Recent reports of Kumar et al. (2025) suggest that Psoralen and Angelicin derivatives show potential dynamic environment when docked with NFkB protein, with a maximum atomic contact of ~89 % with NFkB amino acid residues correlating with observed binding affinity (ΔGbinding) of the molecule 60.92 ± 1.83 kJ/mol, thereby attributing positive impact on BFME phytocompounds in NFkB interactions. The mean Cα RMSDs and their range of standard deviation for the acteoside, glycyrrhizin, hesperidin, myricetin, stevioside, and dexamethasone ranged between 5.6 and 9.8 Å and 5–15 SD, respectively (Srivastava et al., 2024), highlighting the validity of the results derived in the current study.

Tumour necrosis factor-alpha (TNF-α) is an inflammatory cytokine involved in immune regulation, apoptosis, differentiation, proliferation, and development of inflammation. Numerous conditions, such as psoriasis, ankylosing spondylitis, and rheumatoid arthritis, have been connected to TNF-α dysregulation (Inman et al., 2016). Owing to TNF-α′s significant contribution to the inflammatory process, pharmacological development has focused more on inhibiting its activity in recent years. Herein, again, Balanophotannin A has proved to be an effective drug molecule that can interact well with TNF-α due to its predominant lignan glycoside feature that enables higher metabolic activity with inflammatory cytokines (Jiang et al., 2005). Notably, the derived results of the Balanophotannin A and TNF-α TNF-α TNF-α TNF-α complex through molecular dynamics simulations were comparably good to that of the overall structural stability of Calenduloside G methyl ester derived from *Aralia armata,* which exhibited the lowest binding free energy with TNF-α, surpassing the reference inhibitor SPD304 (Le et al., 2025). These findings are consistent with natural polyphenolic compounds exhibiting stable and energetically favorable interactions with TNF-α. Parves et al. (2020) reported RMSD stabilization within 2.5–3.0 Å and consistent hydrogen bonding when evaluating plant-derived inhibitors of TNF-α. Similarly, Khan et al. (2022) demonstrated sustained interaction profiles and low RMSF values in key active-site residues, supporting the stability of TNF-α–ligand complexes under dynamic conditions.

Proinflammatory cytokine Interleukin-6 (IL-6) has a role in the pathogenesis of inflammatory and autoimmune diseases, including COVID-19, cancer, asthma, rheumatoid arthritis, and coronary heart disease. Inflammatory and autoimmune diseases may benefit from treatment targeting IL-6 and its signalling cascade. Based on the study, it can be concluded that Balanophotannin A is biologically significant and a member of the tannin family, which is known to decrease the production of IL-6; it can target IL-6 receptors (Nada et al., 2023). Similarly, Tran et al. (2022) reported RMSD stabilization within 3.0 Å and persistent ligand interactions in their investigation of natural product inhibitors of IL-6. Similarly, Li & Singh (2025) highlighted the dynamic stability and sustained hydrogen bonding in IL-6 complexes, reinforcing the reliability of MD simulations in predicting bioactive inhibitory ligand interactions. A recent study has shown promising and comparable results by the core region of IL-6-chlorogenic acid, which was found to be relatively stable at around or below 0.5 nm, while the ends of the protein changed a lot more during simulation studies (Rajak et al., 2025).

Toll-like receptor 6 (TLR6) is a lipopolysaccharide receptor that triggers pro-inflammatory immune responses to invasive infections. It dimerizes with myeloid differentiation factor 2 (MD2), allowing Toll/IL-1 receptor (TIR) domain-containing adapter protein (TIRAP) to be recruited to the TIR domain of intracellular TLR6 with MyD88. NF-kB is activated as a result of this effect's sequential activation of IL receptor-associated kinase-1/4 (IRAK-1/4). Therefore, it is expected that TLR6/MD2 stimulation of the NF-kB signalling pathway may improve inflammation. Because of this, the research predicts that p-coumaric acid will naturally decrease TLR 6 by lowering malondialdehyde concentration and markedly raising superoxide dismutase levels (Zabad et al., 2019). The derived RMSD of TLR6-p-Coumaric acid complex aligns closely with the findings of Khan et al. (2022), wherein the values for p-Coumaric acid–protein complexes typically were under 2–3 Å over similar timescales. This structural rigidity suggests effective anchoring of the ligand. Ligand torsional angles remained steady, indicating p-Coumaric acid retained a low-energy conformation within the TLR6 binding groove. This conformational stability concurs with findings in MD studies of other phenolic ligands (Rathnayake et al., 2020). According to Mao et al. (2025), germacrone, a bioactive compound from *Radix curcumae* essential oils, has shown similar effects to the derived results in the current study, affirming validation for modulating Toll-like receptors through plant compounds.

The COX enzymes (COX-1 and COX-2) convert arachidonic acid into prostacyclins, thromboxanes, and prostaglandins. COX-1 is constitutively expressed in most tissues, whereas COX-2 is found in just a few tissues and is activated by cytokines and growth

hormones. While COX-1 regulates platelet aggregation and the production of gastrointestinal mucus, COX-2 is implicated in pathological conditions such as inflammation, pain, and fever. Non-steroidal Anti-inflammatory drugs (NSAIDs) work by preventing the COX-1 and COX-2 enzymes from causing inflammation. Based on the docking and simulation data, it is evident that BFME compounds, particularly ellagic acid (EA), may effectively inhibit COX1 because of their strong interaction profile with the COX1 protein (Orlando and Malkowski, 2016). RMSD of Ellagic acid with COX1 receptor remained stable between 1.8 and 2.2 Å. EA with HSP90α, MAPK3, and SRC produced the binding free energy (MM-PBSA) between −39 and −64 kJ/mol (Feifei Sun et al., 2024). EA demonstrated broad target promiscuity with transferrin, kinases (PDK3, MAPK3, SRC, HSP90α), α-amylase, SARS-CoV-2 protease, consistently stabilizing diverse protein systems. According to Amos Tautua et al. (2025), apigenin, a therapeutic phytocompound from *Triumfetta cordifolia,* has shown similar inhibiting effects towards the COX1 enzyme with a comparable dock score of −8.66 kcal/mol with stable hydrogen bonding as witnessed in the COX1 - Ellagic acid complex during simulation. Hence, the present docking and simulation approaches employed in this study have been positive in throwing light on the complex inflammatory cascades and their modulation by BFME compounds through protein interaction and foremost enriched RMSD values.

ADMET analysis is a method for predicting drug development opportunities for natural or synthetic compounds. It can predict around 175 pharmacophores and toxicity attributes. Lipinski's rule of five is used to formulate small molecules for oral use, recommending molecular weights below 750 Da, octanol-water coefficients below 5, and hydrogen donors and acceptors below 5. Furthermore, Jorgenson's rule of three also provides insights into oral bioavailability, as that Lipinski's rule of five (Annadurai et al., 2023). From the results, it can be concluded that Balanophotannin A needs an adjuvant approach to be developed as a novel anti-inflammatory drug, while p-coumaric acid and ellagic acid present in combination with Balanophotannin A in BFME can greatly influence the probable drug efficiency as a synergistic effect. A class of hydrolysable tannins, balanophotannins A-F, from the *Balanophora* species, has raised interest in having a modulating effect on inflammatory responses under various pathological conditions. The anti-inflammatory mechanisms of these compounds have been strictly modulated by suppressing key signaling pathways related to the expression and release of inflammatory cytokines. The inflammatory cytokines, including TNF-α, IL-1β, IL-6, and IFN-γ, are involved in the inflammatory diseases (Wang et al., 2012). All these agents stimulate immune cell recruitment, activating them, increasing reactive oxygen species formation, and enhancing extracellular matrix components' disaggregation. Besides the above, balanophotannin A regulates such increased expressions of these pro-inflammatory cytokines through downregulation at several molecular targets. This is attained by the fact that Balanophotannins inhibit the nuclear factor-kappa B signaling, which mediates inflammation through the blockade of IκBα phosphorylation and degradation, which consequently impairs the nuclear translocation of NF-κB. This would limit the inhibition of transcriptional activation from several pro-inflammatory genes (Wang et al., 2013).

On the other hand, balanophotannins act to modulate the mitogen-activated protein kinase pathway, another integral pathway in the production of inflammatory mediators. By inhibiting phosphorylation of the members of the MAPK family, including p38, ERK1/2, and JNK, balanophotannins reduce TNF-α and IL-6 production and that of other cytokines related to inflammatory response (Jiang et al., 2008). More importantly, such tannins possess antioxidant activity by neutralizing reactive oxygen species, which is in some ways related to further reinforcing inflammatory processes through the activation of the signaling cascade for cytokine production. In fact, by scavenging free radicals, balanophotannins also stabilize cellular environments and further limit inflammation (Wang et al., 2009).

Moreover, balanophotannins have been shown to influence the activities of COX-2 and iNOS up-regulated during inflammation by supporting the synthesis of pro-inflammatory mediators such as prostaglandins and NO. Diminishment of such activities through the counteraction of these enzymes by balanophotannins thus alleviates inflammation (She et al., 2013). Collectively, the multitarget approach of the Balanophotannins mode of action in inflammatory diseases would encompass changes in several key signaling pathways, reduction of oxidative stress, and downregulation of the production of inflammatory cytokines (Ho et al., 2012). These mechanisms place Balanophotannin A among promising candidates for the design of novel anti-inflammatory therapies. Optimization of Balanophotannin A as a prototype drug candidate to be used against inflammatory disorders can also be approached in several ways: optimizing the pharmacokinetic profile and drug-likeness. Such modifications would include, amongst others, lower molecular weight with increased lipophilicity to improve membrane permeability and hence bioavailability. This would, by definition, decrease structural features like the number of hydrogen bond donors and acceptors that may facilitate oral absorption but also blood–brain barrier penetration. Alternatively, prodrug strategies may also be envisaged where a more lipophilic derivative is administered that gets metabolized into an active form of Balanophotannin A in the body. Other important limiting factors are poor water-solubility, instability, or non-targeted delivery that might be mainly solved by nanoparticle encapsulation (or liposome) and decreasing the contribution of systemic exposure to toxicity. It can also potentially improve its pharmacokinetic properties when co-formulated with an absorption enhancer or through other advanced methodologies in a drug delivery system for controlled release rates. In order to lower the possible toxicity due to hERG inhibition, further optimization towards metabolic stability via chemical modification and/or using enzyme inhibitors could enhance the safety profile. Such strategies will further capitalize on the therapeutic potential of Balanophotannin A and render it a more tractable and competitive drug lead for use in inflammatory settings (Fralish et al., 2024; Zawilska et al., 2013; Han and Amidon, 2000; Markovic et al., 2020). Henceforth, BFME can be adopted as a novel prodrug lead against inflammation, considering its molecular mechanisms with inflammation proteins, oral bioavailability, and ADMET properties.

Furthermore, from the findings of croton oil induced ear oedema analysis in rats, it is well established that *B. fungosa* contains immense anti-inflammatory activity. High-dose treatment proved to be the most effective, closely resembling normal ear weight, suggesting strong suppression of croton oil-induced inflammation. Low-dose response was itself comparable to Diclofenac and further supports the pharmacological significance of the extract. Bioactivity of the extract may be contributed by the polyphenols or secondary metabolites, such as coumaric acid, ellagic acid and balanophotannins. P-coumaric acid inhibits inflammatory cytokine production by suppressing NF-κB and MAPK pathways in LPS-stimulated macrophages (Zhao et al., 2016); Ellagic acid has shown remarkable

anti-inflammatory effects in colitis models by downregulation of inflammatory mediators and blockade of signaling pathways like NF-κB and STAT3 (Marín et al., 2013). Previous reports also suggest the anti-inflammatory activity of Balanophotannins, especially those isolated from *B. laxiflora,* which inhibits nitric oxide production and NF-κB activation (Chiou et al., 2011). Hence, such observed dose-related trend and rich phytocompounds profile of *B. fungosa* methanolic extract suggests that it could potentially antagonize pro-inflammatory signal mechanisms, e.g., NF-κB or COX enzyme-mediated pathways. In summary, *B. fungosa* is hence validated to be a promising plant-based anti-inflammatory drug candidate that may support its traditional use and justify future drug development efforts.

5. Limitations and future prospects

This study presents the first pharmacological evidence for *B. fungosa*, demonstrating promising *in vivo* anti-inflammatory activity and identifying Balanophotannin A as a key bioactive compound. While these findings highlight the therapeutic potential of the plant, certain limitations warrant acknowledgment. The isolation and direct experimental validation of Balanophotannin A remain incomplete due to the lack of commercially available standards, and this currently restricts a direct comparison between the isolated compound and the crude extract. Moreover, *in silico* ADMET predictions suggest poor oral absorption and limited blood–brain barrier penetration, which could constrain its development as a conventional orally administered drug. Although molecular docking and 100 ns molecular dynamics simulations confirmed stable protein–ligand interactions, these computational observations require further corroboration through molecular and cellular assays.

Nonetheless, these limitations also open avenues for innovation. Strategies such as nanoparticle-based delivery, prodrug design, or structural analog development could help overcome bioavailability barriers and enhance pharmacological performance. Future work will focus on isolating Balanophotannin A, validating its activity experimentally, and exploring mechanistic pathways. By bridging traditional knowledge with modern pharmacological and technological advances, this study establishes a strong foundation for the future development of *B. fungosa*-based therapeutics against inflammation-related disorders.

6. Conclusion

The current study has opened new avenues for emanating the unexplored anti-inflammatory potential of *B. fungosa* and its therapeutic insights in moderating NF-kB pathway. The bioactivity profile of *B. fungosa* gives tremendous clues in consideration of the multi-dimensional medicinal capabilities for combating inflammation-related disorders. This is greatly attributed to the phytocompounds that need to be isolated further to investigate the mechanism of the bioactivities in an individualistic fashion or following synergism. The bio-accessibility of antioxidant potentials and phytoconstituents release shows remarkable assimilation capabilities *in vitro* that affirm their bioactive food supplementation properties and also warrant further research on the interaction of *B. fungosa* phytocompounds with gut microbiota. The bioactive compounds of *B. fungosa* have been shown to interact efficiently with inflammation proteins through computational methods ie., molecular docking. These findings are consistent with the anti-inflammatory properties of *B. fungosa's* methanolic extract, which has been observed *in vitro* and validated *in vivo*. The drug thus developed from the lead compounds identified in this study backed with *in silico* evidence may pave a new path for the novel performance of natural drugs of anti-inflammatory action, amidst the predominance of NSAIDs and their synthetic associates in the present-day pharmacological uses.

CRediT authorship contribution statement

Gowtham Kannan: Writing – review & editing, Writing – original draft, Visualization, Validation, Methodology, Investigation, Formal analysis, Data curation, Conceptualization. **Benedict Mathews Paul:** Writing – review & editing, Writing – original draft, Visualization, Validation, Formal analysis, Data curation. **Madhu Bala Durairajan:** Writing – review & editing, Formal analysis, Data curation. **Yamuna Annadurai:** Writing – review & editing, Software, Methodology, Formal analysis, Data curation. **Shanmughavel Piramanayagam:** Software, Formal analysis, Data curation. **Parimelazhagan Thangaraj:** Writing – review & editing, Supervision, Resources, Project administration, Funding acquisition, Formal analysis, Data curation.

Ethics and consent

All experimental procedures were conducted in accordance with institutional guidelines and were approved by the Institutional Animal Ethics Committee (IAEC), (Ethics No. KMCRET/ReRc/Ph.D/74/2023), which ensured the ethical compliance of the experiments and the guarantee of animal welfare.

Declaration of competing interest

The authors declare that they have no known competing financial interests or personal relationships that could have appeared to influence the work reported in this paper.

Acknowledgment

Fervent thanks to the Department of Science and Technology – Science and Engineering Research Board (DST-SERB) for the financial grant (File No. EEQ/2021/000203; Dt. March 02, 2022) under DST-SERB-EEQ project for carrying out this research work.

Appendix ASupplementary data

Supplementary data to this article can be found online at https://doi.org/10.1016/j.bcab.2025.103823.

Data availability

Data will be made available on request.

References

Adebayo, S.A., Dzoyem, J.P., Shai, L.J., Eloff, J.N., 2015. The anti-inflammatory and antioxidant activity of 25 plant species used traditionally to treat pain in southern African. BMC Compl. Alternative Med. 15, 1–10. https://doi.org/10.1186/s12906-015-0669-5.

Akbari, B., Baghaei-Yazdi, N., Bahmaie, M., Mahdavi Abhari, F., 2022. The role of plant-derived natural antioxidants in reduction of oxidative stress. Biofactors 48 (3), 611–633. https://doi.org/10.1002/biof.1831.

Amin, E., Abdel-Bakky, M.S., Mohammed, H.A., Hassan, M.H., 2022. Chemical profiling and molecular docking study of *Agathophora alopecuroides*. Life 12 (11), 1852. https://doi.org/10.3390/life12111852.

Amos-tautua, B.M., Ajoko, I.T., Bunu, S.J., 2025. Molecular docking studies of phytochemicals from Triumfetta cordifolia and Spondias mombin against COX-1 and COX-2 enzymes. Asian J. Tropical Biotechnol. 22 (1). https://doi.org/10.13057/biotek/c220105.

Andrade, J.K.S., Barros, R.G.C., Gualberto, N.C., de Oliveira, C.S., Shanmugam, S., Narain, N., 2022. Influence of *in vitro* gastrointestinal digestion and probiotic fermentation on the bioaccessibility of gallic acid and on the antioxidant potential of Brazilian fruit residues. Lwt 153, 112436.

Annadurai, Y., Easwaran, M., Sundar, S., Thangamani, L., Meyyazhagan, A., Malaisamy, A., et al., 2023. SPP1, a potential therapeutic target and biomarker for lung cancer: functional insights through computational studies. J. Biomol. Struct. Dyn. 1–16. https://doi.org/10.1080/07391102.2023.2199871.

Azam, M.N.K., Biswas, P., Khandker, A., Tareq, M.M.I., Tauhida, S.J., Shishir, T.A., et al., 2024. Profiling of antioxidant properties and identification of potential analgesic inhibitory activities of *Allophylus villosus and Mycetia sinensis* employing in vivo, in vitro, and computational techniques. J. Ethnopharmacol., 118695

Bouayed, J., Hoffmann, L., Bohn, T., 2011. Total phenolics, flavonoids, anthocyanins and antioxidant activity following simulated gastro-intestinal digestion and dialysis of apple varieties: bioaccessibility and potential uptake. Food Chem. 128 (1), 14–21. https://doi.org/10.1016/j.foodchem.2011.02.052.

Brodkorb, A., Egger, L., Alminger, M., Alvito, P., Assunção, R., Ballance, S., et al., 2019. INFOGEST static in vitro simulation of gastrointestinal food digestion. Nat. Protoc. 14 (4), 991–1014.

Chanda, J., Mukherjee, P.K., Kar, A., Maitra, P.K., Singha, S., Halder, P.K., et al., 2020. LC–QTOF–MS-based metabolite profiling and evaluation of α-glucosidase inhibitory kinetics of *Coccinia grandis* fruit. Biomed. Chromatogr. 34 (12), e4950. https://doi.org/10.1002/bmc.4950.

Chen, X., Fang, D., Xu, Y., Duan, K., Yoshida, S., Yang, S., et al., 2023. *Balanophora* genomes display massively convergent evolution with other extreme holoparasites and provide novel insights into parasite–host interactions. Nat. Plants 1–16. https://doi.org/10.1038/s41477-023-01517-7.

Chiou, W.F., Shen, C.C., Lin, L.C., 2011. Anti-inflammatory principles from Balanophora laxiflora. J. Food Drug Anal. 19 (4), 20. https://doi.org/10.38212/2224-6614.2216.

Côté, J., Caillet, S., Doyon, G., Sylvain, J.F., Lacroix, M., 2010. Analyzing cranberry bioactive compounds. Crit. Rev. Food Sci. Nutr. 50 (9), 872–888. https://doi.org/10.1080/10408390903042069.

Daroi, P.A., Dhage, S.N., Juvekar, A.R., 2022. p-Coumaric acid mitigates lipopolysaccharide induced brain damage via alleviating oxidative stress, inflammation and apoptosis. J. Pharm. Pharmacol. 74 (4), 556–564. https://doi.org/10.1093/jpp/rgab077.

De Luca, C., Felletti, S., Franchina, F.A., Bozza, D., Compagnin, G., Nosengo, C., et al., 2024. Recent developments in the high-throughput separation of biologically active chiral compounds via high performance liquid chromatography. J. Pharmaceut. Biomed. Anal. 238, 115794. https://doi.org/10.1016/j.jpba.2023.115794.

de Veras, B.O., da Silva, M.V., Ribeiro, P.P.C., 2021. Tannic acid is a gastroprotective that regulates inflammation and oxidative stress. Food Chem. Toxicol. 156, 112482. https://doi.org/10.1016/j.fct.2021.112482.

Dietz, B.M., Hajirahimkhan, A., Dunlap, T., Bolton, J.L., 2016. Botanicals and their bioactive phytochemicals for women's health. Pharmacol. Rev. 68 (4), 1026–1073. https://doi.org/10.1124/pr.115.010843.

Dsvgk, K., Saranya, K.S., Vadlapudi, V., Yarla, N.S., 2014. Evaluation of Anti-inflammatory and Anti-proliferative Activity of Abutilon indicum L. Plant ethanolic leaf extract on lung cancer cell line A549 for system network studies. J. Cancer Sci. Ther. 6, 195–201. https://doi.org/10.4172/1948-5956.1000271.

Durairajan, M.B., Sundararajan, V.V., Kannan, G., Paul, B.M., Muniyandi, K., Thangaraj, P., 2024. Elicitation of nutritional, antioxidant, and antidiabetic potential of barnyard millet (Echinochloa esculenta (A. Braun) H. Scholz) sprouts and microgreens through in vitro bio-accessibility assessment. Food Chem. 441, 138282.

Fralish, Z., Chen, A., Khan, S., Zhou, P., Reker, D., 2024. The landscape of small-molecule prodrugs. Nat. Rev. Drug Discov. 23 (5), 365–380.

Goodsell, D.S., Zardecki, C., Di Costanzo, L., Duarte, J.M., Hudson, B.P., Persikova, I., Segura, J., Shao, C., Voigt, M., Westbrook, J.D., Young, J.Y., Burley, S.K., 2020. RCSB protein Data Bank: enabling biomedical research and drug discovery. Protein Sci.: Publ. Protein Soc. 29 (1), 52–65. https://doi.org/10.1002/pro.3730.

Granado-Serrano, A.B., Martín, M.Á., Bravo, L., Goya, L., Ramos, S., 2012. Quercetin attenuates TNF-induced inflammation in hepatic cells by inhibiting the NF-κB pathway. Nutr. Cancer 64 (4), 588–598. https://doi.org/10.1080/01635581.2012.661513.

Han, H.K., Amidon, G.L., 2000. Targeted prodrug design to optimize drug delivery. AAPS PharmSci 2, 48–58.

Hassan, S.A., Aziz, D.M., Abdullah, M.N., Bhat, A.R., Dongre, R.S., Hadda, T.B., et al., 2023. *In vitro* and *in vivo* evaluation of the antimicrobial, antioxidant, cytotoxic, hemolytic activities and *in silico* POM/DFT/DNA-binding and pharmacokinetic analyses of new sulfonamide bearing thiazolidin-4-ones. J. Biomol. Struct. Dyn. 1–17. https://doi.org/10.1080/07391102.2023.2226713.

Herowati, R., Widodo, G.P., 2017. Molecular docking analysis: interaction studies of natural compounds to anti-inflammatory targets. Quantitative Structure-activity Relationship 63 (10.5772). https://doi.org/10.5772/intechopen.68666.

Ho, S.T., Tung, Y.T., Huang, C.C., Kuo, C.L., Lin, C.C., Yang, S.C., Wu, J.H., 2012. The hypouricemic effect of Balanophora laxiflora extracts and derived phytochemicals in hyperuricemic mice. Evid. base Compl. Alternative Med. 2012 (1), 910152.

Honaiser, T., Arcari, S., Fabiane, K., Rocha, M., Fedrigo, I., Arisi, A., 2022. Synergism and phenolic bioaccessibility during in vitro co-digestion of cooked cowpea with orange juice. Int. J. Food Sci. Technol. 58 (8), 4476–4484. https://doi.org/10.1111/ijfs.16144.

Hu, B., Zhao, X., Zhou, J., Li, J., Chen, J., Du, G., 2023. Efficient hydroxylation of flavonoids by using whole-cell P450 sca-2 biocatalyst in *Escherichia coli*. 2023). Efficient hydroxylation of flavonoids by using whole-cell P450 sca-2 biocatalyst in Escherichia coli. Front. Bioeng. Biotechnol. 11, 1138376. https://doi.org/10.3389/fbioe.2023.1138376.

Huu Tai, B., Xuan Nhiem, N., Hai Yen, P., Hong Quang, T., Thi Cuc, N., Thi Trang, D., et al., 2020. Three new muurolane-type sesquiterpene glycosides from the whole plants of Balanophora fungosa subsp. indica. Natural Product Res. 34 (20), 2964–2970. https://doi.org/10.1080/14786419.2019.1602831.

Inman, R.D., Baraliakos, X., Hermann, K.G.A., Braun, J., Deodhar, A., van der Heijde, D., et al., 2016. Serum biomarkers and changes in clinical/MRI evidence of golimumab-treated patients with ankylosing spondylitis: results of the randomized, placebo-controlled GO-RAISE study. Arthritis Res. Ther. 18 (1), 1–7. https://doi.org/10.1186/s13075-016-1200-1.

Jiang, Z.H., Tanaka, T., Iwata, H., Sakamoto, S., Hirose, Y., Kouno, I., 2005. Ellagitannins and lignan glycosides from *Balanophora japonica* (Balanophoraceae). Chem. Pharm. Bull. 53 (3), 339–341. https://doi.org/10.1248/cpb.53.339.

Jiang, Z.H., Wen, X.Y., Tanaka, T., Wu, S.Y., Liu, Z., Iwata, H., et al., 2008. Cytotoxic hydrolyzable tannins from Balanophora japonica. J. Nat. Prod. 71 (4), 719–723.

Kalaiselvi, V., Vidhya, R., 2015. In-vitro membrane stabilizing activity of different extracts of Bahinia tomentosa (L.) leaves. World J. Pharmaceut. Res. 4 (4), 1700–1715.

Kannan, G., Paul, B.M., Thangaraj, P., 2025. Stimulation, regulation, and inflammaging interventions of natural compounds on nuclear factor kappa B (NF-kB) pathway: a comprehensive review. Inflammopharmacology 1–18.

Karim, M.A., Islam, M.A., Islam, M.M., Rahman, M.S., Sultana, S., Biswas, S., et al., 2020. Evaluation of antioxidant, anti-hemolytic, cytotoxic effects and anti-bacterial activity of selected mangrove plants (*Bruguiera gymnorrhiza* and *Heritiera littoralis*) in Bangladesh. Clin. Phytosci. 6 (1), 1–12. https://doi.org/10.1186/s40816-020-0152-9.

Keen, B., Cawley, A., Reedy, B., Fu, S., 2022. Metabolomics in clinical and forensic toxicology, sports anti-doping and veterinary residues. Drug Test. Anal. 14 (5), 794–807. https://doi.org/10.1002/dta.3245.

Khan, A., Khan, S.U., Khan, A., Shal, B., Rehman, S.U., Rehman, S.U., et al., 2022. Anti-inflammatory and anti-rheumatic potential of selective plant compounds by targeting TLR-4/AP-1 signaling: a comprehensive molecular docking and simulation approaches. Molecules 27 (13), 4319.

Khan, M.S., Althobaiti, M.S., Almutairi, G.S., Alokail, M.S., Altwaijry, N., Alenad, A.M., et al., 2022. Elucidating the binding and inhibitory potential of p-coumaric acid against amyloid fibrillation and their cytotoxicity: biophysical and docking analysis. Biophys. Chem. 291, 106823. https://doi.org/10.1016/j.bpc.2022.106823.

Khatun, M.S., Mia, N., Al Bashera, M., Murad, M.A., Zahan, R., Parvin, S., Akhtar, M.A., 2024. Evaluation of anti-inflammatory potential and GC-MS profiling of leaf extracts from Clerodendrum infortunatum L. J. Ethnopharmacol. 320, 117366.

Kotha, R.R., Tareq, F.S., Yildiz, E., Luthria, D.L., 2022. Oxidative stress and antioxidants—A critical review on *in vitro* antioxidant assays. Antioxidants 11 (12), 2388. https://doi.org/10.3390/antiox11122388.

Kumar, A., Bharadwaj, T., Muthuraj, L., Kumar, J., Kumar, P., Lalitha, R., et al., 2025. Molecular dynamics simulation and docking studies reveals inhibition of NF-kB signaling as a promising therapeutic drug target for reduction in cytokines storms. Sci. Rep. 15 (1), 15225. https://doi.org/10.1038/s41598-024-78411-5.

Le, V.T.T., Tan, L.Q., Hung, D.K., Xuan Ha, N., 2025. Phytochemicals from Aralia armata as potential tumor necrosis factor-alpha inhibitors: a computational study. J. Chem. Res. 49 (3), 17475198251339509. https://doi.org/10.1177/17475198251339509.

Li, Y., Singh, S.P., 2025. Computational screening of IL-1 and IL-6 inhibitors for rheumatoid arthritis: insights from molecular docking and dynamics analysis. Curr. Pharm. Des.

Lin, Y., Luo, T., Weng, A., Huang, X., Yao, Y., Fu, Z., et al., 2020. Gallic acid alleviates gouty arthritis by inhibiting NLRP3 inflammasome activation and pyroptosis through enhancing Nrf2 signaling. Front. Immunol. 11, 580593.

Lu, X., Gu, X., Shi, Y., 2022. A review on lignin antioxidants: their sources, isolations, antioxidant activities and various applications. Int. J. Biol. Macromol. 210, 716–741. https://doi.org/10.1016/j.ijbiomac.2022.04.228.

Luo, B., Zou, K., Wang, H., Tang, Z.C., Yu, L.L., 2007. Studies on chemical constituents of *Balanophora involucrata*. Li Shizhen Med Materia Medica Res. 18, 1929–1930.

Malherbe, C.J., De Beer, D., Joubert, E., 2012. Development of on-line high performance liquid chromatography (HPLC)-biochemical detection methods as tools in the identification of bioactives. Int. J. Mol. Sci. 13 (3), 3101–3133. https://doi.org/10.3390/ijms13033101.

Mali, S.N., Chaudhari, H.K., 2019. Molecular modelling studies on adamantane-based Ebola virus GP-1 inhibitors using docking, pharmacophore and 3D-QSAR. SAR QSAR Environ. Res. 30 (3), 161–180.

Mamani-Huanca, M., de la Fuente, A.G., Otero, A., Gradillas, A., Godzien, J., Barbas, C., López-Gonzálvez, Á., 2021. Enhancing confidence of metabolite annotation in Capillary Electrophoresis-mass spectrometry untargeted metabolomics with relative migration time and in-source fragmentation. J. Chromatogr. A 1635, 461758.

Mamani-Huanca, M., Gradillas, A., López-Gonzálvez, Á., Barbas, C., 2022. In-source fragmentation for the identification of compounds by CE-ESI-TOF in human plasma. L-proline as case study. In: Capillary Electrophoresis-Mass Spectrometry: Methods and Protocols. Springer US, New York, NY, pp. 185–202.

Mao, Z., Lin, X., Hu, Y., Liu, Y., Yu, S., Zhou, T., et al., 2025. Exploring the anti-inflammatory effects of Radix Curcumae essential oil in pulmonary sarcoidosis via the TLR4/MyD88/NF-κB pathway. Phytomedicine, 156496. https://doi.org/10.1016/j.phymed.2025.156496.

Mariadoss, A.V.A., Park, S., Saravanakumar, K., Sathiyaseelan, A., Wang, M.H., 2023. Phytochemical profiling, *in vitro* antioxidants, and antidiabetic efficacy of ethyl acetate fraction of *Lespedeza cuneata* on streptozotocin-induced diabetic rats. Environ. Sci. Pollut. Control Ser. 1–18. https://doi.org/10.1007/s11356-023-26412-8.

Marín, M., Giner, R.M., Ríos, J.L., Recio, M.C., 2013. Intestinal anti-inflammatory activity of ellagic acid in the acute and chronic dextrane sulfate sodium models of mice colitis. J. Ethnopharmacol. 150 (3), 925–934. https://doi.org/10.1016/j.jep.2013.09.030.

Markovic, M., Ben-Shabat, S., Dahan, A., 2020. Prodrugs for improved drug delivery: lessons learned from recently developed and marketed products. Pharmaceutics 12 (11), 1031.

Martínez, J.E.B., Concha, D.D.R.M., Velázquez, T.G.G., Martínez, C.J., Ruiz, J.C.R., 2021. Anti-inflammatory properties of phenolic extracts from Phaseolus vulgaris and Pisum sativum during germination. Food Biosci. 42, 101067.

Melo, P., Massarioli, A., Lazarini, J., Soares, J., Franchin, M., Rosalen, P., et al., 2020. Simulated gastrointestinal digestion of brazilian açaí seeds affects the content of flavan-3-ol derivatives, and their antioxidant and anti-inflammatory activities. Heliyon 6 (10), e05214. https://doi.org/10.1016/j.heliyon.2020.e05214.

Minekus, M., Alminger, M., Alvito, P., Ballance, S., Bohn, T., Bourlieu, C., Carrière, F., Boutrou, R., Corredig, M., Dupont, D., Dufour, C., Egger, L., Golding, M., Karakaya, S., Kirkhus, B., Le Feunteun, S., Lesmes, U., Macierzanka, A., Mackie, A., Marze, S., McClements, D.J., M?nard, O., Recio, I., Santos, C.N., Singh, R.P., Vegarud, G.E., Wickham, M.S.J., Weitschies, W., Brodkorb, A., et al., 2014. A standardised static in vitro digestion method suitable for food–an international consensus. Food Funct. 5 (6), 1113–1124.

Moskaug, J.Q., Carlsen, H., Myhrstad, M.C.W., Blomhoff, R., 2005. Polyphenols and glutathione synthesis regulation. Am. J. Clin. Nutr. 81 (Suppl. l), 277–283.

Mutinda, E.S., Zhang, D.J., Muema, F.W., Mkala, E.M., Waswa, E.N., Odago, W.O., et al., 2023. The genus balanophora JR Forst. –Its use in traditional medicine, phytochemistry, and pharmacology: a review. J. Ethnopharmacol., 117276

Nada, H., Sivaraman, A., Lu, Q., Min, K., Kim, S., Goo, J.I., Lee, K., 2023. Perspective for discovery of small molecule IL-6 inhibitors through Study of structure–activity relationships and molecular docking. J. Med. Chem. 66 (7), 4417–4433. https://doi.org/10.1021/acs.jmedchem.2c01957.

Nandiyanto, A.B.D., Oktiani, R., Ragadhita, R., 2019. How to read and interpret FTIR spectroscope of organic material. Indonesian J. Sci. Technol. 4 (1), 97–118.

Nangap, M.J.T., Walbadet, L., Mbock, M.A., Adjieufack, A.I., Ongagna, J.M., Fokou, R., et al., 2024. In vitro, in vivo and in silico antiplasmodial profiling of the aqueous extract of Hibiscus asper HOOK F. Leaf (Malvaceae). J. Ethnopharmacol. 335, 118536.

Nataraj, G., Jagadeesan, G., Manoharan, A.L., Muniyandi, K., Sathyanarayanan, S., Thangaraj, P., 2023. Ipomoea pes-tigridis L. extract accelerates wound healing in Wistar albino rats in excision and incision models. J. Ethnopharmacol. 317, 116808.

Nguyen, T.D., Do, T.H., Tran, V.T.H., Nguyen, H.A., Pham, D.V., 2022. Anti-inflammatory effect of a triterpenoid from *Balanophora laxiflora*: results of bioactivity-guided isolation. Heliyon 8 (3), e09070, 1214.

Nieto, J., Fernández-Jalao, I., Siles-Sánchez, M., Santoyo, S., Jaime, L., 2023. Implication of the polymeric phenolic fraction and matrix effect on the antioxidant activity, bioaccessibility, and bioavailability of grape stem extracts. Molecules 28 (6), 2461. https://doi.org/10.3390/molecules28062461.

Nweze, C.C., Tsea, W., Ekpe, I.P., 2022. Anti-Inflammatory properties of quercetin: a review. J. Drug Deliv. Therapeut. 12 (4). https://doi.org/10.22270/jddt.v12i4.5453.

Orlando, B.J., Malkowski, M.G., 2016. Crystal structure of rofecoxib bound to human cyclooxygenase-2. Acta Crystallogr. F: Struct. Biol. Commun. 72 (10), 772–776. https://doi.org/10.1107/S2053230X16014230.
Pan, J., Zhang, S., Yan, L., Tai, J., Xiao, Q., Zou, K., Zhou, Y., Wu, J., 2008. Separation of flavanone enantiomers and flavanone glucoside diastereomers from *Balanophora involucrate* Hook. f. by capillary electrophoresis and reversed-phase high-performance liquid chromatography on a 18 column. J. Chromatogr. A 1185 (1), 117–129.
Parimelazhagan, T., 2015. Pharmacological Assays of Plant-based Natural Products, vol. 71. Springer. https://doi.org/10.1007/978-3-319-26811-8.
Parves, M.R., Mahmud, S., Riza, Y.M., Sujon, K.M., Uddin, M.A.R., Chowdhury, M.I.A., et al., 2020. Inhibition of TNF-alpha using plant-derived small molecules for treatment of inflammation-mediated diseases. In: Proceedings. MDPI, 79, No. 1, p. 13.
Paul, B.M., Jagadeesan, G., Kannan, G., Raj, F.J., Annadurai, Y., Piramanayagam, S., Thangaraj, P., 2024. Exploring the hypoglycaemic efficacy of bio-accessed antioxidative polyphenolics in thermally processed *Cucumis dipsaceus* fruits–An *in vitro*and *in silico* study. Food Chem. 435, 137577. https://doi.org/10.1016/j.foodchem.2023.137577.
Peron, G., Phuyal, G.P., Hošek, J., Adhikari, R., Dall'Acqua, S., 2024. Identification of hydroxyquinazoline alkaloids from Justicia adhatoda L. leaves, a traditional natural remedy with NF-κB and AP-1-mediated anti-inflammatory properties and antioxidant activity. J. Ethnopharmacol. 331, 118345.
Pierce, R., Ogle, C., 2017. Musky Rat Kangaroos and other vertebrates feeding from the flowers of the root parasite 'Balanophora fungosa'. North Queensland Naturalist 47, 14–20.
Piesche, M., Roos, J., Kühn, B., Fettel, J., Hellmuth, N., Brat, C., et al., 2020. The emerging therapeutic potential of nitro fatty acids and other Michael acceptor-containing drugs for the treatment of inflammation and cancer. Front. Pharmacol. 11, 1297. https://doi.org/10.3389/fphar.2020.01297.
Raina-Fulton, R., Mohamad, A.A., 2018. Pressurized solvent extraction with ethyl acetate and liquid chromatography—tandem mass spectrometry for the analysis of selected conazole fungicides in Matcha. Toxics 6 (4), 64. https://doi.org/10.3390/toxics6040064.
Rajagopal, K., Varakumar, P., Baliwada, A., Byran, G., 2020. Activity of phytochemical constituents of Curcuma longa (turmeric) and Andrographis paniculata against coronavirus (COVID-19): an in-silico approach. Future J. Pharmaceut. Sci. 6, 1–10. https://doi.org/10.1186/s43094-020-00126-x.
Rajak, P., Ganguly, A., Dey, S., Sen, K., Banerjee, M., Mukherjee, A., 2025. In silico study unravels the inhibitory potential of phenolic acids against the Interleukin-6 and TNF-α: revealing the route to anti-inflammatory effects. Food and Humanity, 100615. https://doi.org/10.1016/j.foohum.2025.100615.
Ranjithakani, P., Geetha, S., Lakshmi, G., Murugan, S., 1992. Preliminary survey of wild edibles of Kolli Hills of Salem Ancient Science of. Life 11, 133–136.
Rathnayake, S., Madushanka, A., Wijegunawardana, N.D., Mylvaganam, H., Rathnayake, A., Perera, E.G., et al., 2020. In silico study of 5, 7-dimethoxycoumarin and p-coumaric acid in Carica papaya leaves as dengue virus type 2 protease inhibitors. Multidisciplinary Digital Publishing Institute Proceedings 79 (1), 11.
Rezaei, Z., Momtaz, S., Gharazi, P., Rahimifard, M., Baeeri, M., Abdollahi, A.R., et al., 2024. Cinnamic acid ameliorates acetic acid-induced inflammatory response through inhibition of TLR-4 in colitis rat model. Anti-Inflammatory & anti-allergy agents in medicinal chemistryrrent medicinal chemistry-anti-inflammatory and anti-allergy agents), 23(1), 21-30. https://doi.org/10.2174/0118715230278980231212103709.
Rosnack, K.J., Reid, M.J., Ladak, A., Cleland, G., 2016. Screening solution using the software platform UNIFI: an integrated workflow by waters. In: Assessing Transformation Products of Chemicals by Non-target and Suspect Screening– Strategies and Workflows. Volume 2 (pp. 155–172). American Chemical Society.
Sandor, M., Kiss, R., Keseru, G.M., 2010. Virtual fragment docking by Glide: a validation study on 190 protein–fragment complexes. J. Chem. Inf. Model. 50 (6), 1165–1172.
Saxena, S., Abdullah, M., Sriram, D., Guruprasad, L., 2018. Discovery of novel inhibitors of Mycobacterium tuberculosis MurG: homology modelling, structure based pharmacophore, molecular docking, and molecular dynamics simulations. J. Biomol. Struct. Dyn. 36 (12), 3184–3198.
Schulz, M., Biluca, F.C., Gonzaga, L.V., Borges, G.D.S.C., Vitali, L., Micke, G.A., et al., 2017. Bioaccessibility of bioactive compounds and antioxidant potential of juçara fruits (Euterpe edulis Martius) subjected to in vitro gastrointestinal digestion. Food Chem. 228, 447–454.
Seke, F., Manhivi, V., Slabbert, M., Sultanbawa, Y., Sivakumar, D., 2022. In vitro release of anthocyanins from microencapsulated natal plum (carissa macrocarpa) phenolic extract in alginate/psyllium mucilage beads. Foods 11 (17), 2550. https://doi.org/10.3390/foods11172550.
She, G.M., Zhang, Y.J., Yang, C.R., 2009. Phenolic constituents from Balanophora laxiflora with DPPH radical-scavenging activity. Chem. Biodivers. 6 (6), 875–880.
She, G.M., Zhang, Y.J., Yang, C.R., 2013. A new phenolic constituent and a cyanogenic glycoside from Balanophora involucrata (Balanophoraceae). Chem. Biodivers. 10 (6), 1081–1087.
Shinde, U.A., Phadke, A.S., Nair, A.M., Mungantiwar, A.A., Dikshit, V.J., Saraf, M.N., 1999. Membrane stabilizing activity—a possible mechanism of action for the anti-inflammatory activity of Cedrus deodara wood oil. Fitoterapia 70 (3), 251–257.
Silva, A.D., Ávila, S., Küster, R.T., Dos Santos, M.P., Grassi, M.T., de Queiroz Pereira Pinto, C., et al., 2021. In vitro bioaccessibility of proteins, phenolics, flavonoids and antioxidant activity of Amaranthus viridis. Plant Foods Hum. Nutr. 76, 478–486.
Socrates, G., 2004. Infrared and Raman Characteristic Group Frequencies: Tables and Charts. John Wiley & Sons.
Srivastava, A.K., Srivastava, S., Kumar, V., Ghosh, S., Yadav, S., Malik, R., et al., 2024. Identification and mechanistic exploration of structural and conformational dynamics of NF-kB inhibitors: rationale insights from in silico and in vitro studies. J. Biomol. Struct. Dyn. 42 (3), 1485–1505.
Sun, Feifei, Liu, Jinde, Xu, Jingfei, Ali, Tariq, Wu, Yongning, Lin, Li, 2024. Molecular mechanism of yi-qi-yang-yin-ye against obesity in rats using network pharmacology, molecular docking, and molecular dynamics simulations. Arab. J. Chem. 17 (1), 105390. https://doi.org/10.1111/jcmm.1796, 10.1016/j.arabjc.2023.105390.
Surh, Y., 2011. Reverse pharmacology applicable for botanical drug development – inspiration from the legacy of traditional wisdom. J. Tradit. Complement. Med. 1 (1), 5–7. https://doi.org/10.1016/s2225-4110(16)30051-7.
Thilakarathna, R.C.N., Siow, L.F., Tang, T.K., Chan, E.S., Lee, Y.Y., 2023. Physicochemical and antioxidative properties of ultrasound-assisted extraction of mahua (*Madhuca longifolia*) seed oil in comparison with conventional Soxhlet and mechanical extractions. Ultrason. Sonochem. 92, 106280. https://doi.org/10.1016/j.ultsonch.2022.106280.
Thummajitsakul, S., Samaikam, S., Tacha, S., Silprasit, K., 2020. Study on FTIR spectroscopy, total phenolic content, antioxidant activity and anti-amylase activity of extracts and different tea forms of *Garcinia schomburgkiana* leaves. Lwt 134, 110005. https://doi.org/10.1016/j.lwt.2020.110005.
Tian, C., Liu, X., Chang, Y., Wang, R., Yang, M., Liu, M., 2021. Rutin prevents inflammation induced by lipopolysaccharide in RAW 264.7 cells via conquering the TLR4-MyD88-TRAF6-NF-κB signalling pathway. J. Pharm. Pharmacol. 73 (1), 110–117.
Tran, Q.H., Nguyen, Q.T., Vo, N.Q.H., Mai, T.T., Tran, T.T.N., Tran, T.D., et al., 2022. Structure-based 3D-Pharmacophore modeling to discover novel interleukin 6 inhibitors: an in silico screening, molecular dynamics simulations and binding free energy calculations. PLoS One 17 (4), e0266632.
Tubaro, A., Dri, P., Delbello, G., Zilli, C., Della Loggia, R., 1986. The croton oil ear test revisited. Agents Actions 17, 347–349. https://doi.org/10.1007/BF01982641.
Tung, N.T., Hung, N.Q., Luyen, N.T., Dat, N.T., Püssa, T., Rusalepp, L., Raal, A., 2021. Chemical constituents and biological activities of Balanophora fungosa varietas globosa growing in Vietnam, as well as comparative chromatography with some species of the genus Balanophora JR & G. Forst. Proc. Est. Acad. Sci. 70 (1), 40–50. https://doi.org/10.3176/proc.2021.1.01.
Wang, W., Zeng, S.F., Yang, C.R., Zhang, Y.J., 2009. A new hydrolyzable tannin from Balanophora harlandii with radical-scavenging activity. Helv. Chim. Acta 92 (9), 1817–1822.
Wang, X., Liu, Z., Qiao, W., Cheng, R., Liu, B., She, G., 2012. Phytochemicals and biological studies of plants from the genus Balanophora. Chem. Cent. J. 6, 1–9.
Wang, Y., Yang, J., Wang, A., Ma, J., Tian, J., Ji, T., Su, Y., 2013. Hydrolyzable tannins from Balanophora polyandra. Acta Pharm. Sin. B 3 (1), 46–50.
Wisetkomolmat, J., Arjin, C., Hongsibsong, S., Ruksiriwanich, W., Niwat, C., Tiyayon, P., et al., 2023. Antioxidant activities and characterization of polyphenols from selected Northern Thai rice husks: relation with seed attributes. Rice Sci. 30 (2), 148–159. https://doi.org/10.1016/j.rsci.2023.01.007.
Xia, Q., Wang, L., Xu, C., Mei, J., Li, Y., 2017. Effects of germination and high hydrostatic pressure processing on mineral elements, amino acids and antioxidants in vitro bioaccessibility, as well as starch digestibility in brown rice (Oryza sativa L.). Food Chem. 214, 533–542.
Yao, L., Cheng, S., Yang, J., Xiang, F., Zhou, Z., Zhang, Q., et al., 2022. Metabolomics reveals the intervention effect of Zhuang medicine Longzuantongbi granules on a collagen-induced arthritis rat model by using UPLC-MS/MS. J. Ethnopharmacol. 294, 115325.
Zabad, O.M., Samra, Y.A., Eissa, L.A., 2019. P-Coumaric acid alleviates experimental diabetic nephropathy through modulation of toll like receptor-4 in rats. Life Sci. 238, 116965. https://doi.org/10.1016/j.lfs.2019.116965.

Zawilska, J.B., Wojcieszak, J., Olejniczak, A.B., 2013. Prodrugs: a challenge for the drug development. Pharmacol. Rep. 65 (1), 1–14.
Zhang, C., 2023. Therapeutic mechanisms of ellagic acid for inflammation and related conditions. In: International Conference on Modern Medicine and Global Health (ICMMGH 2023), 2789, pp. 703–708. SPIE.
Zhang, P., Liu, N., Xue, M., Zhang, M., Liu, W., Xu, C., et al., 2023. Anti-inflammatory and antioxidant properties of β-sitosterol in copper sulfate-induced inflammation in zebrafish (Danio rerio). Antioxidants 12 (2), 391.
Zhao, Y., Liu, J., Liu, C., Zeng, X., Li, X., Zhao, J., 2016. Anti-inflammatory effects of p-coumaric acid in LPS-stimulated RAW264. 7 cells: involvement of NF-κB and MAPKs pathways. Med. Chem. 6, 327–330. https://doi.org/10.4172/2161-0444.1000365.
Zhao, H., Yang, Y., Wang, S., Yang, X., Zhou, K., Xu, C., et al., 2023. NPASS database update 2023: quantitative natural product activity and species source database for biomedical research. Nucleic Acids Res. 51 (D1), D621–D628. https://doi.org/10.1093/nar/gkac1069.
Zhou, J., Du, S.Y., Fang, Z.Y., Zeng, Z., 2021. New butenolides with anti-inflammatory activity from *Balanophora fungosa*. Nat. Prod. Res. 35 (11), 1825–1829. https://doi.org/10.1080/14786419.2019.1645663.